ATF4, the primary inducer of *Eif4ebp1* under ER stress, is activated by translational suppression by eIF2α phosphorylation during the acute phase. We found that 4E-BP1 protein is stable with a half-life of approximately 20 hr (Figure S6). Thus, 4E-BP1 protein seems to continue to be expressed abundantly during the later stages of the UPR. This is consistent with the recent observation that several prosurvival proteins involved in the UPR are stable, while proapoptotic proteins are not (Rutkowski et al., 2006). We found that global protein synthesis was higher in 4E-BP1-deficient β cells than in wild-type cells under ER stress conditions. In particular, expression of CHOP was augmented in 4E-BP1 deficiency. Enhanced CHOP expression in 4E-BP1-deficient cells suggests that a reduction in eIF4E availability due to 4E-BP1 induction suppresses CHOP translation during ER stress in wild-type cells, possibly accounting for one of the mechanisms by which 4E-BP1 plays a role in adaptation to ER stress. Important roles of translational control via eIF4E availability have also been suggested in prolonged hypoxia (Koritzinsky et al., 2006). However, the signaling mechanisms for translational control are different: ER stress increases 4E-BP1 protein levels via ATF4 in β cells, while hypoxia enhances 4E-BP1 activity via dephosphorylation and also causes eIF4E nuclear localization in HeLa cells.

The present results also suggest that variations in genes regulating eIF4E availability and/or eIF4F formation may have an impact on susceptibility to diabetes. In this context, a recent report demonstrating that a gene encoding eIF4A2, a component of eIF4F, is possibly linked to type 2 diabetes in French families (Cheyssac et al., 2006) is of great interest. Furthermore, our findings raise the possibility that 4E-BP1 may be a potential target for diabetes mellitus treatment.

EXPERIMENTAL PROCEDURES

Animal Experiments

All animal experiments were approved by the Tohoku University Institutional Animal Care and Use Committee. *Wfs1*$^{-/-}$ mice were backcrossed to a 129S6 (Taconic) background for six generations. *Ins2*$^{WT/C96Y}$ mice (Charles River Laboratories) were backcrossed to a 129S6 background for five generations. *Eif4ebp1*$^{-/-}$ mice were maintained on a 129S6 background. Only male mice were used. For the in vivo studies shown in Figures 4A, 4C, and 4D, littermates from crosses of male *Ins2*$^{WT/C96Y}$ *Eif4ebp1*$^{+/-}$ and female *Ins2*$^{WT/WT}$ *Eif4ebp1*$^{+/-}$ mice were used. For Figures 4B, 4E, and 4F, littermates from intercrosses of *Eif4ebp1*$^{+/-}$ *Wfs1*$^{+/+}$ mice and littermates from intercrosses of *Eif4ebp1*$^{+/-}$ *Wfs1*$^{-/-}$ mice were used. For isolated islet experiments (Figures 4G and 4H), age-matched nonlittermate mice were used. To induce ER stress in vivo, mice were given a 0.5 μg/g body weight intraperitoneal injection of tunicamycin. After 96 hr, kidneys and livers were removed. Tissue sample processing, immunostaining of pancreatic sections, and determination of β cell area and pancreatic insulin content were performed as described previously (Ishihara et al., 2004).

Cell Culture and Cell Viability Assay

Pancreatic tumors in *Eif4ebp1*$^{-/-}$:SV40Tag mice on a mixed background were excised, yielding MIN6*Eif4ebp1*$^{-/-}$ cells, which were used at 5–10 passages in this study. MIN6 cells were cultured in DMEM supplemented with 15% FCS. *Atf4*$^{-/-}$ MEFs were cultured in DMEM supplemented with a nonessential amino acid mixture and 10% FCS. Cells seeded in 24-well plates 2 days previously were treated with thapsigargin or tunicamycin and used for western blotting or cell viability assay. Cell viability was determined with a cell proliferation assay kit (Promega). Construction of adenoviruses and infection of MIN6 cells were performed as described previously (Ishihara et al., 2004).

Northern and Western Blotting and Cap-Binding Affinity Assay

Total RNA extracted using ISOGEN (Nippon Gene) was probed with ^{32}P-labeled cDNAs. Tissue homogenates and cell lysates were subjected to SDS-PAGE and probed with primary antibodies against 4E-BP1, 4E-BP2, eIF4E, eIF4G, cleaved caspase-3 (Cell Signaling), ATF4, CHOP (Santa Cruz), and actin (Sigma). Cell lysates were incubated with 7-methyl-GTP (^{7}mGTP)-Sepharose (Amersham) overnight at 4°C. The ^{7}mGTP-Sepharose was then pelleted and boiled. Experiments were performed at least three times. Band intensity was quantified using Scion Image software.

Metabolic Labeling

Due to the low islet yields from *Ins2*$^{WT/C96Y}$, *Ins2*$^{WT/C96Y}$ *Eif4ebp1*$^{-/-}$, *Wfs1*$^{-/-}$, and *Eif4ebp1*$^{-/-}$ *Wfs1*$^{-/-}$ mice, islets with these genotypes were pooled from two or three mice. Fifty to eighty islets were cultured for 3 days in RPMI supplemented with 10% FCS. Islets washed with methionine/cysteine-free RPMI containing 10% dialyzed FCS were labeled with a protein labeling mix (PerkinElmer) (1.0 MBq/tube) for 15 min and then resolved in sample buffer (1.0 μl/islet for wild-type and *Eif4ebp1*$^{-/-}$ islets and 0.75 μl/islet for other genotypes). The level of protein synthesis was quantified from autoradiograms. For measurement of *Chop* translation, 4 × 10^6 cells treated with thapsigargin for 12 hr were washed with methionine/cysteine-free DMEM containing 15% dialyzed FCS and labeled with [^{35}S]methionine/cysteine (20 MBq/bottle) for 2 hr. Cells were then resolved in lysis buffer (50 mM Tris [pH 7.5], 150 mM NaCl, 2 mM $MgCl_2$, 0.1% Triton X-100, and protease inhibitors [Roche]). Lysates were precleared with Protein A Sepharose Fast Flow (Amersham) and incubated with anti-CHOP antibody (R-20, Santa Cruz) overnight.

Firefly Luciferase Reporter Assay

Oligonucleotides containing ATF4 binding sites were annealed and subcloned into the pGL3-Promoter vector (BamHI-SalI, Promega). MIN6 cells were transfected with luciferase reporters using Lipofectamine (Invitrogen). Luciferase activity was assayed with a dual-luciferase system (Promega) using a luminometer (Berthold).

Chromatin Immunoprecipitation Assay

Proteins bound to DNA were crosslinked with 1% formaldehyde at 4°C for 20 min. After sonication, the protein-DNA complexes were immunoprecipitated using an anti-ATF4 antibody (C-20, Santa Cruz). After reversal of the crosslinks at 65°C for 6 hr, DNA was purified on a DNA purification column (QIAGEN). PCR was performed with the primers 5′-GATGAGGAAGAGGAAGCTGAGT TG-3′ and 5′-AGTTGTAAGAGGAGTAGTTGGGGG-3′.

Statistical Analysis

Data are presented as means ± SEM. Differences between groups were assessed by Student's t test. $p < 0.05$ was considered significant.

SUPPLEMENTAL DATA

Supplemental Data include six figures and Supplemental References and can be found with this article online at http://www.cellmetabolism.org/cgi/content/full/7/3/269/DC1/.

ACKNOWLEDGMENTS

We thank J. Alam (Alton Ochsner Medical Foundation) and D. Ron (New York University) for their generous gifts of DN-ATF4 cDNA and *Atf4*$^{-/-}$ MEFs, respectively. We are also grateful to K. Igarashi (Tohoku University) for advice on ChIP analysis and to Y. Nagura and K. Tanaka for their expert technical assistance. This work was supported by Grants-in-Aid for Scientific Research

(H) [^{35}S]methionine/cysteine labeling as in (G) in islets of the indicated genotypes at 6–8 weeks of age. Lane 1, wild-type; lane 2, *Eif4ebp1*$^{-/-}$; lane 3, *Wfs1*$^{-/-}$; lane 4, *Eif4ebp1*$^{-/-}$ *Wfs1*$^{-/-}$. Data from three experiments are summarized in the right panel. *$p < 0.05$.
Error bars represent SEM.

(19590300 to H.I. and 19209034 to Y.O.) from the Ministry of Education, Culture, Sports, Science and Technology of Japan.

Received: July 10, 2007
Revised: December 2, 2007
Accepted: January 30, 2008
Published: March 4, 2008

REFERENCES

Butler, A.E., Janson, J., Bonner-Weir, S., Ritzel, R., Rizza, R.A., and Butler, P.C. (2003). β-cell deficit and increased beta-cell apoptosis in humans with type 2 diabetes. Diabetes *52*, 102–110.

Cheyssac, C., Dina, C., Lepretre, F., Vasseur-Delannoy, V., Dechaume, A., Lobbens, S., Balkau, B., Ruiz, J., Charpentier, G., Pattou, F., et al. (2006). EIF4A2 is a positional candidate gene at the 3q27 locus linked to type 2 diabetes in French families. Diabetes *55*, 1171–1176.

Clemens, M.J. (2001). Translational regulation in cell stress and apoptosis. Roles of the eIF4E binding proteins. J. Cell. Mol. Med. *5*, 221–239.

Delepine, M., Nicolino, M., Barrett, T., Golamaully, M., Lathrop, G.M., and Julier, C. (2000). EIF2AK3, encoding translation initiation factor 2-alpha kinase 3, is mutated in patients with Wolcott-Rallison syndrome. Nat. Genet. *25*, 406–409.

Harding, H.P., Novoa, I., Zhang, Y., Zeng, H., Wek, R., Schapira, M., and Ron, D. (2000). Regulated translation initiation controls stress-induced gene expression in mammalian cells. Mol. Cell *6*, 1099–1108.

Harding, H.P., Zeng, H., Zhang, Y., Jungries, R., Chung, P., Plesken, H., Sabatini, D.D., and Ron, D. (2001). Diabetes mellitus and exocrine pancreatic dysfunction in perk−/− mice reveals a role for translational control in secretory cell survival. Mol. Cell *7*, 1153–1163.

Harding, H.P., Zhang, Y., Zeng, H., Novoa, I., Lu, P.D., Calfon, M., Sadri, N., Yun, C., Popko, B., Paules, R., et al. (2003). An integrated stress response regulates amino acid metabolism and resistance to oxidative stress. Mol. Cell *11*, 619–633.

He, C.H., Gong, P., Hu, B., Stewart, D., Choi, M.E., Choi, A.M., and Alam, J. (2001). Identification of activating transcription factor 4 (ATF4) as an Nrf2-interacting protein. Implication for heme oxygenase-1 gene regulation. J. Biol. Chem. *276*, 20858–20865.

Holcik, M., and Sonenberg, N. (2005). Translational control in stress and apoptosis. Nat. Rev. Mol. Cell Biol. *6*, 318–327.

Ibrahimo, S., Holmes, L.E., and Ashe, M.P. (2006). Regulation of translation initiation by the yeast eIF4E binding proteins is required for the pseudohyphal response. Yeast *23*, 1075–1088.

Inoue, H., Tanizawa, Y., Wasson, J., Behn, P., Kalidas, K., Bernal-Mizrachi, E., Mueckler, M., Marshall, H., Donis-Keller, H., Crock, P., et al. (1998). A gene encoding a transmembrane protein is mutated in patients with diabetes mellitus and optic atrophy (Wolfram syndrome). Nat. Genet. *20*, 143–148.

Ishihara, H., Takeda, S., Tamura, A., Takahashi, R., Yamaguchi, S., Takei, D., Yamada, T., Inoue, H., Soga, H., Katagiri, H., et al. (2004). Disruption of the WFS1 gene in mice causes progressive beta-cell loss and impaired stimulus-secretion coupling in insulin secretion. Hum. Mol. Genet. *13*, 1159–1170.

Koritzinsky, M., Magagnin, M.G., van den Beucken, T., Seigneuric, R., Savelkouls, K., Dostie, J., Pyronnet, S., Kaufman, R.J., Weppler, S.A., Voncken, J.W., et al. (2006). Gene expression during acute and prolonged hypoxia is regulated by distinct mechanisms of translational control. EMBO J. *25*, 1114–1125.

Laybutt, D.R., Preston, A.M., Akerfeldt, M.C., Kench, J.G., Busch, A.K., Biankin, A.V., and Biden, T.J. (2007). Endoplasmic reticulum stress contributes to beta cell apoptosis in type 2 diabetes. Diabetologia *50*, 752–763.

Miyazaki, J., Araki, K., Yamato, E., Ikegami, H., Asano, T., Shibasaki, Y., Oka, Y., and Yamamura, K. (1990). Establishment of a pancreatic beta cell line that retains glucose-inducible insulin secretion: special reference to expression of glucose transporter isoforms. Endocrinology *127*, 126–132.

Novoa, I., and Carrasco, L. (1999). Cleavage of eukaryotic translation initiation factor 4G by exogenously added hybrid proteins containing poliovirus 2Apro in HeLa cells: effects on gene expression. Mol. Cell. Biol. *19*, 2445–2454.

Novoa, I., Zeng, H., Harding, H.P., and Ron, D. (2001). Feedback inhibition of the unfolded protein response by GADD34-mediated dephosphorylation of eIF2α. J. Cell Biol. *153*, 1011–1022.

Pirot, P., Naamane, N., Libert, F., Magnusson, N.E., Orntoft, T.F., Cardozo, A.K., and Eizirik, D.L. (2007). Global profiling of genes modified by endoplasmic reticulum stress in pancreatic beta cells reveals the early degradation of insulin mRNAs. Diabetologia *50*, 1006–1014.

Riggs, A.C., Bernal-Mizrachi, E., Ohsugi, M., Wasson, J., Fatrai, S., Welling, C., Murray, J., Schmidt, R.E., Herrera, P.L., and Permutt, M.A. (2005). Mice conditionally lacking the Wolfram gene in pancreatic islet beta cells exhibit diabetes as a result of enhanced endoplasmic reticulum stress and apoptosis. Diabetologia *48*, 2313–2321.

Rutkowski, D.T., Arnold, S.M., Miller, C.N., Wu, J., Li, J., Gunnison, K.M., Mori, K., Sadighi Akha, A.A., Raden, D., and Kaufman, R.J. (2006). Adaptation to ER stress is mediated by differential stabilities of pro-survival and pro-apoptotic mRNAs and proteins. PLoS Biol. *4*, e374.

Scheuner, D., Mierde, D.V., Song, B., Flamez, D., Creemers, J.W., Tsukamoto, K., Ribick, M., Schuit, F.C., and Kaufman, R.J. (2005). Control of mRNA translation preserves endoplasmic reticulum function in β cells and maintains glucose homeostasis. Nat. Med. *11*, 757–764.

Schroder, M., and Kaufman, R.J. (2005). The mammalian unfolded protein response. Annu. Rev. Biochem. *74*, 739–789.

Strom, T.M., Hortnagel, K., Hofmann, S., Gekeler, F., Scharfe, C., Rabl, W., Gerbitz, K.D., and Meitinger, T. (1998). Diabetes insipidus, diabetes mellitus, optic atrophy and deafness (DIDMOAD) caused by mutations in a novel gene (wolframin) coding for a predicted transmembrane protein. Hum. Mol. Genet. *7*, 2021–2028.

Teleman, A.A., Chen, Y.W., and Cohen, S.M. (2005). 4E-BP functions as a metabolic brake used under stress conditions but not during normal growth. Genes Dev. *19*, 1844–1848.

Tettweiler, G., Miron, M., Jenkins, M., Sonenberg, N., and Lasko, P.F. (2005). Starvation and oxidative stress resistance in Drosophila are mediated through the eIF4E-binding protein, d4E-BP. Genes Dev. *19*, 1840–1843.

Tsukiyama-Kohara, K., Poulin, F., Kohara, M., DeMaria, C.T., Cheng, A., Wu, Z., Gingras, A.C., Katsume, A., Elchebly, M., Spiegelman, B.M., et al. (2001). Adipose tissue reduction in mice lacking the translational inhibitor 4E-BP1. Nat. Med. *7*, 1128–1132.

Wang, J., Takeuchi, T., Tanaka, S., Kubo, S.K., Kayo, T., Lu, D., Takata, K., Koizumi, A., and Izumi, T. (1999). A mutation in the insulin 2 gene induces diabetes with severe pancreatic β-cell dysfunction in the Mody mouse. J. Clin. Invest. *103*, 27–37.

Zhang, P., McGrath, B., Li, S., Frank, A., Zambito, F., Reinert, J., Gannon, M., Ma, K., McNaughton, K., and Cavener, D.R. (2002). The PERK eukaryotic initiation factor 2α kinase is required for the development of the skeletal system, postnatal growth, and the function and viability of the pancreas. Mol. Cell. Biol. *22*, 3864–3874.

Available online at www.sciencedirect.com
ScienceDirect
Neuroscience Research 61 (2008) 143–158
Neuroscience Research
www.elsevier.com/locate/neures

Behavioral and gene expression analyses of *Wfs1* knockout mice as a possible animal model of mood disorder

Tadafumi Kato [a,*], Mizuho Ishiwata [a], Kazuyuki Yamada [b], Takaoki Kasahara [a], Chihiro Kakiuchi [a], Kazuya Iwamoto [a], Koki Kawamura [c], Hisamitsu Ishihara [d], Yoshitomo Oka [d]

[a] *Laboratory for Molecular Dynamics of Mental Disorders, RIKEN Brain Science Institute, Hirosawa 2-1, Wako, Saitama 351-0198, Japan*
[b] *Support Unit for Animal Experiment, RIKEN Brain Science Institute, Wako, Saitama 351-0198, Japan*
[c] *Laboratory for Cell Culture Development, RIKEN Brain Science Institute, Wako, Saitama 351-0198, Japan*
[d] *Division of Molecular Metabolism and Diabetes, Tohoku University Graduate School of Medicine, Sendai, Japan*

Received 21 November 2007; accepted 7 February 2008
Available online 14 February 2008

Abstract

Wolfram disease is a rare genetic disorder frequently accompanying depression and psychosis. Non-symptomatic mutation carriers also have higher rates of depression and suicide. Because *WfS1*, the causative gene of Wolfram disease, is located at 4p16, a linkage locus for bipolar disorder, mutations of *WfS1* were suggested to be involved in the pathophysiology of bipolar disorder. In this study, we performed behavioral and gene expression analyses of *Wfs1* knockout mice to assess the validity as an animal model of mood disorder. In addition, the distribution of *Wfs1* protein was examined in mouse brain. *Wfs1* knockout mice did not show abnormalities in circadian rhythm and periodic fluctuation of wheel-running activity. Behavioral analysis showed that *Wfs1* knockout mice had retardation in emotionally triggered behavior, decreased social interaction, and altered behavioral despair depending on experimental conditions. *Wfs1*-like immunoreactivity in mouse brain showed a similar distribution pattern to that in rats, including several nuclei potentially relevant to the symptoms of mood disorders. Gene expression analysis showed down-regulation of *Cdc42ep5* and *Rnd1*, both of which are related to Rho GTPase, which plays a role in dendrite development. These findings may be relevant to the mood disorder observed in patients with Wolfram disease.

Keywords: Wolframin; Wolfram disease; Depression; Bipolar disorder; DNA microarray; Forced swimming test

1. Introduction

Wolfram disease (Online Mendelian Inheritance in Man [OMIM] 222300) is a rare autosomal recessive neurodegenerative disorder characterized by early-onset diabetes mellitus, progressive optic atrophy, diabetes insipidus, and deafness (Domenech et al., 2006); *WfS1/wolframin* has been identified as the causative gene (Strom et al., 1998; Inoue et al., 1998). Approximately, 60% of the patients with Wolfram disease have mental symptoms, such as severe depression, psychosis, impulsivity, and aggression (Swift et al., 1990). More importantly, carriers of *WfS1* mutations, who are not affected with Wolfram disease, have a 26-fold higher likelihood of psychiatric hospitalization mainly due to depression (Swift and Swift, 2000). The *WfS1* gene locates at 4p16.1 (Strom et al., 1998; Inoue et al., 1998), a replicated linkage locus of bipolar disorder (Ewald et al., 1998, 2002; Detera-Wadleigh et al., 1999). Some studies showed that bipolar disorder with psychosis (Als et al., 2004; Cheng et al., 2006) or suicidal behavior (Cheng et al., 2006) is linked with this locus. These lines of evidence suggested the possible role of *WfS1* mutations in the pathophysiology of bipolar disorder and related phenotypes.

To date, mutation screening of the *WfS1* gene has been reported in 84 patients with bipolar disorder, 54 with major depression, 119 with schizophrenia, 100 suicide victims, 3 with schizoaffective disorder, and several other patients with other psychiatric diagnoses (Ohtsuki et al., 2000; Martorell et al., 2003; Torres et al., 2001; Crawford et al., 2002; Evans et al., 2000). However, none of these patients had mutations causing Worfram disease.

* Corresponding author. Tel.: +81 48 467 6949; fax: +81 48 467 6947.
E-mail address: kato@brain.riken.jp (T. Kato).

0168-0102/$ – see front matter © 2008 Published by Elsevier Ireland Ltd and the Japan Neuroscience Society.
doi:10.1016/j.neures.2008.02.002

Despite the fact that *WfS1* mutations may not be a frequent cause of mental disorders, the mechanism underlying how *WfS1* mutations lead to mental symptoms in patients with Wolfram disease will shed light on the pathophysiology of mood disorders. Mice lacking the *Wfs1* gene might be useful as a genetic animal model of mood disorders.

The symptoms of Wolfram disease resemble those of mitochondrial diseases and, indeed, initial studies suggested mitochondrial dysfunction in Wolfram disease based on mitochondrial DNA (mtDNA) deletions found in patients (Rotig et al., 1993). However, the protein coded by *WfS1* was found to be localized in endoplasmic reticulum (ER) (Takeda et al., 2001; Philbrook et al., 2005). *WfS1* expression was induced by ER stress (Fonseca et al., 2005) or *XBP1* overexpression (Kakiuchi et al., 2006), and disruption of *Wfs1* caused a dysfunctional ER stress response (Fonseca et al., 2005; Riggs et al., 2005; Yamada et al., 2006). Recent studies have provided insight into the function of *WfS1* protein; *WfS1* induces cation channel activity on ER membranes (Osman et al., 2003) and regulates calcium levels in ER (Takei et al., 2006). It also plays a role in stimulus-secretion coupling for insulin exocytosis in pancreatic β cells (Ishihara et al., 2004). Disruption of *Wfs1* increased vulnerability to cell death in the knockout (KO) mice (Ishihara et al., 2004; Philbrook et al., 2005; Riggs et al., 2005; Yamada et al., 2006). In the rat brain, *WfS1* was distributed predominantly in neurons of the so-called limbic system (Takeda et al., 2001). *WfS1* mutations could lead to loss of *WfS1*-expressing neurons in particular brain regions of patients with Wolfram disease, which may underlie progression of mental symptoms.

In this study, we performed behavioral analysis of *Wfs1* KO mice to characterize their behavioral abnormality. We previously developed neuron-specific mutant polymerase γ-transgenic mice (mPolg Tg mice) based on a mitochondrial dysfunction hypothesis of bipolar disorder (Kato and Kato, 2000) and demonstrated that these mice had bipolar disorder-like phenotypes, such as altered circadian rhythm and periodic fluctuation of wheel-running activity (Kasahara et al., 2006). Whether or not the *Wfs1* KO mice show such wheel-running activity was examined. A behavioral test battery was also conducted to search for other behavioral phenotypes. Distribution of *Wfs1* in the brain was examined to search for the neural basis of behavioral alteration. In addition, gene expression analysis was performed to search for the molecular basis of behavioral phenotypes of *Wfs1* KO mice.

2. Experimental procedures

2.1. Generation of Wfs1 KO mice

The methods for the generation of *Wfs1* KO mice have been described elsewhere (Ishihara et al., 2004). In brief, a neomycin-resistance gene was inserted into exon 2 of the *Wfs1* gene in the targeting vector. The targeting vector was injected into 129Sv embryonic stem (ES) cells, and the ES cells with homologous recombination were obtained. By crossing the chimeric mice with C57BL/6J (B6) mice, *Wfs1* heterozygous KO mice were obtained. Genotyping was performed as previously described (Ishihara et al., 2004). The heterozygous KO mice were crossed with the B6 mice for at least eight generations before the analysis. The mice were maintained in a 12-h light:12-h dark cycle, except for several specific experiments as indicated. Wild-type (WT) littermates were used for the control whenever possible. All animal experiments were approved by the local animal experiment committees of RIKEN and Behavioral and Medical Sciences Research Consortium (BMSRC) (Akashi, Japan). Animal experiments were carried out in accordance with the National Institute of Health Guide for the Care and Use of Laboratory Animals. All efforts were made to minimize the number of animals used and their suffering.

2.2. Wheel-running activity

For this analysis, 11 homozygous KO mice ($Wfs1^{-/-}$) and 9 WT littermates ($Wfs1^{+/+}$) were used. All were males aged 34 weeks at the initiation of the analysis. The groups did not differ significantly in body weight.

The methods for the analysis of wheel-running activity were described in detail elsewhere (Kasahara et al., 2006). In brief, mice were individually housed in cages (width, 24 cm; depth, 11 cm; height, 14 cm) equipped with a steel wheel (width, 5 cm; diameter, 14 cm) (O'Hara & Co., Tokyo, Japan). Wheel-running activity was monitored by measuring the rotation of the wheel (3 counts/1 rotation). Food and water were available ad libitum. The data of initial 7–10 days were omitted from the analysis. Delayed and anticipatory activity indices, referring to the wheel-running activity during the initial 3 h of a light phase and that during the last 3 h of a light phase, were calculated. The periodicity of wheel-running activity was assessed by Lomb-Scargle periodogram (Kasahara et al., 2006).

The Mann–Whitney *U*-test was used for statistical analyses. Significance levels were set at 0.05 (two-tailed; d.f., degree of freedom). The average and standard error of mean (S.E.M.) were presented for each experimental parameter in one group.

2.3. Behavioral analysis: phase I. Screening by a test battery

This analysis was performed at BMSRC (Akashi, Japan). For this analysis, 14 homozygous KO mice ($Wfs1^{-/-}$), 14 heterozygous KO mice ($Wfs1^{-/+}$), and 13 WT littermates ($Wfs1^{+/+}$) were analyzed. All were males aged 12 weeks at the initiation of the behavioral analysis. The analyses were performed in the order of open-field test, startle response and prepulse inhibition test, elevated plus maze, Morris water maze, passive avoidance learning, active avoidance learning, and forced swimming test. After the behavioral test battery, the non-fasting blood glucose level was examined to rule out the possibility that elevated blood glucose levels might affect the results of behavioral analysis. There was no significant difference among the genotypes, consistent with a previous report that there was no apparent increase in blood glucose levels in *Wfs1* KO mice on the B6 background (Ishihara et al., 2004).

2.3.1. Open-field test

A transparent cubic box without a ceiling (30 cm × 30 cm × 30 cm) was placed in a ventilated sound-attenuating chamber. A 40-W white lamp provided room lighting, which was approximately 110 lx on the floor of the chamber. In addition, a fan attached on the upper part of the wall at one end of the chamber presented a masking noise of 45 dB. Two infrared beams were set on each wall 2 cm above the floor with an interval of 10 cm. The total number of successive interceptions of two adjoining beams on each bank was scored as locomotion behavior. The other 12 infrared ray beams were attached 4.5 cm above the floor in 2.5-cm intervals, and the total number of vertical beam interceptions was scored as rearing behavior. Each mouse was allowed to explore freely in the open-field area for 20 min.

For statistical analysis, repeated measures analysis of variance (ANOVA) with the intrasubject factor of time (1–20 min) and the intersubject factor of genotype (−/−, +/−, and +/+) was applied.

2.3.2. Startle response and prepulse inhibition (PPI)

Each mouse was enclosed in a transparent acrylic box (7 cm × 7 cm × 10 cm). Startle response was detected as vibration of the box, using an accelerometer (GH-313A, Keyence, Osaka, Japan). The acoustic startle pulse of broadband burst (115 dB, 50 ms) and tone prepulse (85 dB, 30 ms) were presented via a speaker located in front of the box. Light prepulse (30 ms) was

applied by LED. At the beginning of the session, 40 startle pulses were presented to test for basal startle responsiveness and its habituation. The average values of eight blocks, consisting of five startle pulses each, were used for the statistical analysis. After that, three different types of trials were performed: startle pulse alone (n = 12), startle pulse preceded by a tone prepulse (n = 12), and startle pulse preceded by a light prepulse (n = 12). Prepulses were presented 50, 100, or 200 ms before the startle pulse. In total, six types of prepulse (n = 4, each) were applied. The mean interval averaged 25 s (15–45 s) throughout the session. The startle response was recorded for 200 ms with the sampling frequency of 1000 Hz. The PPI was assessed by the ratio of the mean response of trials with one type of prepulse (n = 4) divided by the mean response of trials without prepulse (n = 12). Because light prepulse did not attenuate the startle response at all, only the data of tone prepulse were presented.

2.3.3. Elevated plus maze

The maze consisted of four arms, two open arms and two closed arms, 5 cm wide and 30 cm long with a gray acrylic floor, that met at a 10 cm × 10 cm center zone. Two closed arms had the transparent walls of 15 cm height on both sides, and the open arms had the low walls of 3 mm height on the both sides. The apparatus was mounted 75 cm above the floor of the room. The room lighting was approximately 20 lx on the maze. The video camera was placed 80 cm above the maze. A fan generated a masking noise of 45 dB. The animal was placed gently onto the center of the maze and was allowed to explore the maze freely for 10 min. Number of entries into each arm and time spent in each arm were recorded from videotapes.

2.3.4. Morris water maze

A round pool, with the diameter of 95 cm and the depth of 21.5 cm, was placed in the center of a 140 cm × 130 cm room. A platform with the diameter of 11 cm was set in one of quadrants and 5 mm beneath the surface of black water maintained at 21 ± 1 °C. On the first to fifth days, five trials per day were performed for learning phase. The mouse was released on one of three quadrants of the pool without the platform, and the time to reach the platform was measured. When the mouse could not reach the platform within 60 s, the experimenter placed the mouse on the platform. On the sixth day, a probe test was performed to examine whether the mouse remembered the place of the platform. The mouse was released in the quadrant on the opposite side of the platform and its behavior for 60 s was videotaped. The time staying in the target quadrant, where the platform had been placed, and immobility time were measured.

2.3.5. Passive avoidance learning

A mouse was placed in a box, consisting of two rooms separated by a shutter, that is, light and dark compartments (10 cm × 10 cm each). In the acquisition trial, the mouse was kept in the light compartment. Five seconds later, the door to the dark compartment was opened. When the mouse moved into the dark compartment, the shutter was closed, and 10 s later, an electrical shock (160 V, 3 s) was delivered through the grid floor. Twenty-four hours later, each mouse was placed again in the light compartment and the latency to enter the dark compartment was recorded up to a maximum of 180 s.

2.3.6. Active avoidance learning

The same apparatus with the one used for passive avoidance learning was used, but there was no shutter between the light and dark compartments. The box was set in a soundproof chamber, and illuminated by a 20 W white light set on the chamber. The ceiling of the dark room is made of a black acryl board, and the ceiling of the light room was a transparent acryl board.

The training was performed for 3 days. On each day, one session consisting of 50 trials was performed. In each trial, a condition stimulus (CS) of 1500 Hz sound (85 dB) was followed by an unconditioned stimulus (US) of 140-V electrical shock. The US was given 5 s after the initiation of the CS and continued until the mouse escaped to the other compartment. If the mouse did not move to the other compartment, the US lasted 15 s together with the CS. If the mouse moved within 5 s after the CS, CS was stopped and no US was given. None of the mice experienced the maximum length of the CS. The time from the CS to the escape and the number of escapes were used for the performance of learning.

2.3.7. Forced swimming test

Animals were thrown into a square pool 24 cm × 24 cm in size. The water was maintained constant at 21 °C. On the first day, the mice were left in the pool for 20 min, and the mobility during the first 5 min recorded by videocamera was assessed. On the second day, animals were thrown into the pool for 5 min and the immobility time during the 5 min was recorded. The immobility was defined by the two criteria. (1) No movement of all legs and the tail. (2) Completely stationary state in the pool, or the movement only by inertia by the adjacent movement. The immobility was assessed by three independent raters by scrutinizing the video and the median value of the three raters was used for the analysis.

2.4. Behavioral analysis: phase II

This analysis was performed at the Support Unit for Animal Experiment, RIKEN BSI. For this analysis, 9 homozygous KO mice ($Wfs1^{-/-}$) and 11 WT littermates ($Wfs1^{+/+}$) were analyzed. All were males aged 31 weeks at the initiation of the behavioral analysis. There was no significant difference of body weight at the initiation of the behavioral tests.

The analyses were performed in the order of home cage activity, open-field test, light-dark (L-D) box test, elevated plus maze, startle response and PPI test, Morris water maze, and fear conditioning. After each trial (except the auditory startle response and the water maze), apparatuses were wiped and cleaned by 80% alcohol and damp towel. For data acquisition, the Image J program (http://rsb.info.Nih.gov/ij) was used after some modification.

2.4.1. Environment of behavioral laboratory and housing condition of mice

Mice were housed individually for several days before they were transferred to the behavioral laboratory. The laboratory was air-conditioned and maintained temperature and humidity within approximately 22–23 °C and 50–55%. Food and water were freely available except during experimentation. Large tweezers were used to handle mice to avoid individual differences in the handling procedure. All of the experiments were conducted in the light phase (9:00–18:00 h), and the starting times of the experiments were kept constant.

2.4.2. Home cage activity measurement

Spontaneous activity of mice in their home cage was measured using a 24-ch ABsystem 4.0 (Neuroscience, Tokyo, Japan). Cages were individually set into the compartments made of stainless steel in the negative pressure rack (JCL, Tokyo, Japan). An infrared sensor was equipped on the ceiling of each compartment and it detected movements of the mice. Home cage activity was measured for 1 week from the afternoon of the day of transferring to the behavioral laboratory (day 1) until the next day of the week (day 8). After the termination of home cage activity measurement, cages and bedding materials were changed to fresh ones and then mice were maintained in the micro-isolation rack (Allentown Inc., Allentown, PA, USA), the same as those used in breeding rooms throughout the behavioral screening.

2.4.3. Open-field test

Four days after the termination of home cage activity measurement (day 12), an open-field test was conducted. The detailed protocol is shown in the supplementary information.

2.4.4. L-D box test

The next day (day 13) after the open-field test, an L-D box test was conducted. A four-channel of the L-D box system was equipped in the same sound-proof room as the open field. Each light box was made of white plastic (20 cm × 20 cm × 20 cm [H]) and illuminated by LEDs (250 lx at the center of the box); a CCD camera was equipped on the ceiling. Each dark box was made of black plastic (20 cm × 20 cm × 20 cm [H]) and an infrared camera was equipped on the ceiling. There was a tunnel for transition on the center panel between the light box and dark box (3 cm × 5 cm) with an automatic sliding door. In the L-D box test, mice were individually introduced into the light box, and the door of the tunnel automatically opened 3 s after the introduction of a mouse. Then mouse was allowed to move freely in the L-D box for 10 min. Total distance traveled, percent distance traveled in the light

box, percent duration staying in the light box, numbers of the transition between light and dark box, and the first latency to enter the dark box were measured as indices.

2.4.5. Elevated plus maze test

The next day (day 14) after the L-D box test, an elevated plus maze test was conducted. The detailed protocol is shown in the supplementary information.

2.4.6. Auditory startle response

The next day after the L-D box test, an auditory startle response test was conducted for 2 days. The detailed protocol is shown in the supplementary information.

2.4.7. The Morris water maze test

Three days after the termination of the auditory startle response test (day 18), a series of the Morris water maze test began. The detailed protocol is shown in the supplementary information.

2.4.8. Classical fear conditioning

Three days after the termination of the Morris water maze test (day 25), a classical fear-conditioning test was conducted. This test consisted of three parts: a conditioning trial (day 25), a context test trial (day 26), and a cued test trial (day 27). Fear conditioning was carried out on a clear plastic chamber equipped with a stainless steel grid floor (34 cm × 26 cm × 30 cm [H]). A CCD camera was equipped on the ceiling of the chamber and was connected to a video monitor and computer. The grid floor was wired to a shock generator. White noise (65 dB) was supplied from a loudspeaker as an auditory cue (CS). The conditioning trial consisted of a 2-min exploration period followed by two CS-US pairings separated by 1 min each. A US (foot-shock: 0.5 mA, 2 s) was administered at the end of the 30-s CS period. A context test was performed in the same conditioning chamber for 3 min in the absence of the white noise at 24 h after the conditioning trial. Further, a cued test was performed in an alternative context with distinct cues; the test chamber was different from the conditioning chamber in brightness (almost 0–1 lx), color (white), floor structure (no grid), and shape (triangular). The cued test was conducted 24 h after the contextual test was finished and consisted of a 2-min exploration period (no CS) to evaluate the non-specific contextual fear followed by a 2-min CS period (no foot shock) to evaluate the acquired cued fear. Rate of freezing response of mice was measured as an index of fear memory.

2.5. Behavioral analysis: phase III

This analysis was performed at the Support Unit for Animal Experiment, RIKEN BSI. For this analysis, seven homozygous KO mice (*Wfs1*$^{-/-}$) and eight WT littermates (*Wfs1*$^{+/+}$) were analyzed. All were males aged 9 weeks at the initiation of the behavioral analysis. There was no significant difference of body weight at the initiation of the behavioral tests (WT, 25.2 ± 0.6 g; KO, 25.2 ± 0.5 g).

The analyses were performed in the order of social interaction, rotarod test, sucrose preference test, tail suspension test, forced swimming test, marble burying test, hot plate test, and tail flick test. Inter-test intervals were 1 day to a week. After each trial (except the auditory startle response and the water maze), apparatuses were wiped and cleaned by 80% alcohol and damp towel. For data acquisition, the Image J program was used after some modification.

2.5.1. Social interaction test (encounter method)

Subject mice were individually put into the center of a white-colored open field (40 cm × 40 cm × 30 cm [H]). Immediately after the introduction of the subject mouse, a target mouse was also introduced into the same open field. The duration of contact behavior was measured for 60 min to assess passive contact. Contact or separation of mice was expressed as "1" or "2" by computerized image analysis. If the two mice contacted, the software return value of "1," and if separated, return value "2." Thus, smaller number means higher contact. Data were collected and analyzed using a personal computer and commercially available software (Time HC; O'Hara, Tokyo, Japan).

2.5.2. Motor coordination and motor learning test (rotarod)

Mice were individually placed on a rotating rod (O'Hara, Tokyo, Japan) and the time each animal was able to maintain its balance walking on top of the rod was measured. The speed of the rotarod was 4 rpm (on the first day) or accelerated from 4 to 40 rpm over a 4-min period and 40 rpm another 1 min (day 2 to day 5). Mice were given a trial for 2 min (day 1) or four trials with a maximum time of 300 s (inter-trial intervals were 20–30 s). Time between placement and falling or revolving around the rod was recorded manually.

2.5.3. Sucrose preference test

Mice were tested for a 3-days 24-h test and 1-day 1-h test with water deprivation. The 24-h tests were free choice between two bottles, one with sucrose (3% in filtered water) and another with filtered water. To eliminate the side preference, the position of bottles was switched every 24 h. The consumption of water and sucrose solution was assessed daily. After the choice test, mice were deprived water for 24 h and then a 1-h choice test between water and sucrose was conducted.

2.5.4. Tail suspension test

Mice were individually hung by the tail using an adhesive tape placed approximately 1.5 cm from the tip of the tail attached to a wire and 30 cm above the floor. The duration of immobility was scored and analyzed using Image J TS (O'Hara, Tokyo, Japan) for 5 min.

2.5.5. Forced swimming test

Mice were individually placed for 15 min (day 1) or 5 min (day 2) in glass cylinders (30 cm high, 10 cm in diameter) containing 10 cm of water maintained at 23–25 °C. The duration of immobility was scored and analyzed using Image J software. The immobility time during the first 5 min was assessed.

2.5.6. Marble burying test

The test was performed in the test cage identical to their home cage with a 5-cm thick layer of bedding material (TEK-FRESH, Edstrom Industries, Waterford, WI, USA). Mice were habituated to fresh bedding for 30 min and then briefly returned to their home cage; 20 glass marbles (1.5 cm in diameter) were placed evenly on the bedding. Mice were then reintroduced into the test cage and the number of buried marbles (buried into the bedding over 2/3) was analyzed 30 min later.

2.5.7. Hot plate and tail flick test

In the hot plate test (Model MK-350C, Muromachi-kikai, Tokyo, Japan), mice were individually placed on the plate (52 ± 0.5 °C) enclosed in a translucent plastic wall, and the time between placement and licking of the paws and jumping was recorded manually as the response latency. A cut-off time was 90 s. Because most of the mice did not jump, latency to licking was used for statistical analysis.

In the tail flick test (Model MK-330B, Muromachi-kikai, Tokyo, Japan), mice were individually restricted on the radiant heat meter and focused heat was applied to the surface of the tail at 2–3 cm from its tip; the latency to reflexive removal of the tail from the heat was recorded manually as the tail flick latency. A cut-off time was 10 s.

In these tests, data were obtained by two observers, and the shorter scores were adopted as the response time.

2.5.8. Statistical analysis

For statistical analysis of behavioral analyses phases I–III, the Student's *t*-test, one-way ANOVA, and repeated measures ANOVA (RMANOVA) were used. When a significant effect was found by one-way ANOVA, Tukey post hoc comparisons were applied. When sphericity was rejected by the Mauchly test before the application of RMANOVA, the Greenhouse-Geisser estimate was used. Paired *t*-test and two-sample *t*-test were also used for post hoc analysis when necessary. These statistical analyses were performed using SPSS 11.0 for Windows (SPSS Japan, Tokyo, Japan). Significance levels were set at 0.05 (two-tailed); d.f., degree of freedom. Average and standard error of mean (S.E.M.) were presented for each experimental parameter in one group.

2.6. Immunohistochemistry

Because several computer programs predicted that mouse *Wfs1* protein would be cleaved around position 36, we used the following amino acid sequence, Glu^{39}–Gly^{53} as an antigen. A hexadecapeptide (CEPPRAPRPQADPSAG) was synthesized, purified using high-performance liquid chromatography, and conjugated to keyhole limpet hemocyanin (KLH). Five Balb/c mice were injected intraperitoneally with the KLH-conjugated peptide emulsified in complete Freund's adjuvant. Antiserum was obtained 1 week after boosting with the same antigen. We performed Western blot analysis to selected sensitive antiserum specific to *Wfs1* protein.

For immunohistochemical analysis using *WfS1* antibody, wild-type B6 mice aged 20–22 weeks were used. The mouse brain was fixed by perfusion of paraformaldehyde and embedded with paraffin. Coronal or sagittal sections with the thickness of 8 μm were sliced from paraffin-embedded mouse brain.

After deparaffinization and hydration, the slices were incubated for 10 min at 95 °C in sodium citrate buffer. Endogenous peroxidase activity was quenched by H_2O_2/methanol treatment. For blocking, 0.8% Block Ace (Dainippon Sumitomo Pharma, Osaka, Japan) in phosphate-buffered saline (PBS) was used. Anti-*WfS1* antiserum was used by 2500× dilution. For second antibody, biotinylated anti-mouse IgG (Vector Laboratories, Burlingame, CA, USA) was used. Peroxidase/DAB staining was performed by Vectastain Elite ABC kit (Vector Laboratories).

2.7. DNA microarray analysis

DNA microarray analysis was performed in two developmental stages, 12 and 30 weeks old. Eight homozygous *Wfs1* KO mice and 8 WT littermates were sacrificed at the age of 12 weeks. Seven homozygous *Wfs1* KO mice and five WT littermates were also analyzed at the age of 30 weeks.

The hippocampus was rapidly dissected, and total RNA samples were extracted from the hippocampi using TRIzol reagent (Invitrogen, Carlsbad, CA, USA). Microarray analysis was performed according to the manufacturer's protocol (Affymetrix, Santa Clara, CA, USA). Briefly, 5 μg total RNA of each sample was reverse-transcribed into cDNA, and biotinylated cRNA was synthesized from the cDNA by in vitro transcription. DNA microarray experiments were performed using Mouse Genome 430 2.0 GeneChips (Affymetrix). The hybridization signal on the chip was scanned by a GeneArray scanner and processed by GeneSuite software (Affymetrix). The probe sets labeled as "present" in 8 of 16 samples at 12 weeks old (24703/45101 probe sets) or in 5 of 12 samples at 30 weeks old (24455/45101 probe sets) were selected. The raw data were analyzed using MAS5 (Affymetrix) and then imported into GeneSpring 7.3 software (Silicon Genetics, Redwood, CA). The signal intensity of each probe set on the microarray was divided by its median value using GeneSpring 7.3 software.

For statistical analysis, the Mann–Whitney *U*-test was performed between the KO mice and their WT littermates, and $P < 0.05$ was considered statistically significant.

The probe sets were classified based on the information from GeneOntology (http://www.geneontology.org/) using GeneSpring software. For the GeneOntology analysis, the differentially expressed probes were selected. The categories showing overrepresentation at the level of $P < 0.05$ and containing 10 or more probe sets were selected.

2.8. Real-time quantitative polymerase chain reaction (RT-PCR) analysis

The representative probe sets that showed altered expression in the DNA microarray analysis of mouse brains were verified by RT-PCR. The cDNA used for the DNA microarray analysis was used. Primers and probes for Gapdh, cdc42ep5, Rnd1, Wnt2, and Garnl1 were commercially available by the Assay-on-Demand service (Applied Biosystems, Foster City, CA). The assays were carried out according to the protocols supplied by the manufacturer using 7900HT real-time PCR systems (Applied Biosystems). The relative values were calculated by measuring $\Delta C_t = C_t$ (each gene) $- C_t$ (Gapdh) for each sample in quadruplicate. For statistical analysis, one-tailed Mann–Whitney *U*-test was applied, and $P < 0.05$ was considered statistically significant.

3. Results

3.1. Wheel-running activity

To assess whether or not the *Wfs1* KO mice show bipolar disorder-like behavioral phenotypes, wheel-running activity of the *Wfs1* KO mice and WT littermates was recorded for a period up to 2 months. The levels of wheel-running activity and the circadian rhythm were assessed using male mice that were 34 weeks old at the initiation of this analysis (KO, $n = 11$; WT, $n = 9$). Average wheel-running activity per day of *Wfs1* KO mice during 28 days under the L-D condition did not differ from that of WT littermates (Fig. 1a; WT, 221.3 ± 64.7 [mean ± S.E.M.] counts; KO, 142.2 ± 57.6 counts, d.f. = 18, $U = 29$, $P = 0.21$ by Mann-Whitney *U*-test). Delayed activity

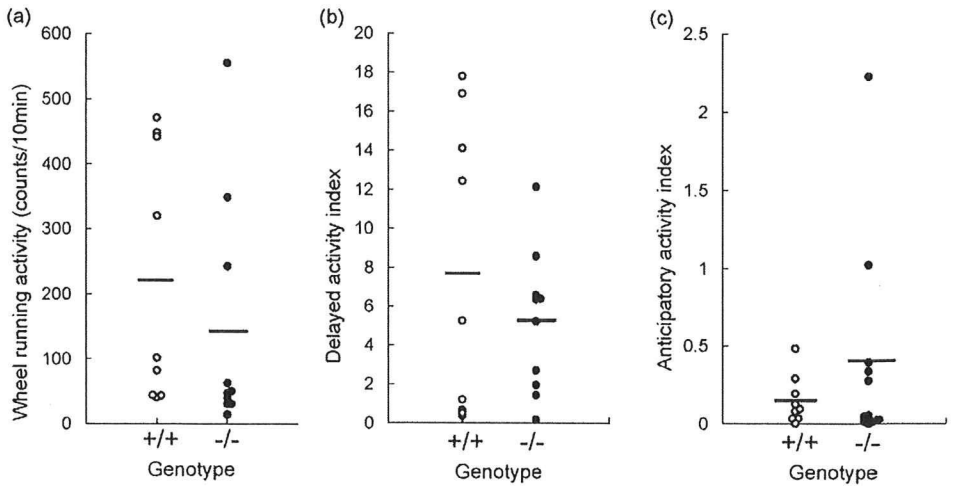

Fig. 1. Long-term wheel-running activity analysis. (a) Wheel-running activity. (b) Delayed activity index. Delayed activity index is defined as a percent of the wheel-running activity during the first 3 h of the light period with the total activity during the previous dark period (12 h). (c) Anticipatory activity index, the wheel-running activity in the last 3 h of light phase in comparison with the activity during dark phase. +/+, WT mice; −/−, *Wfs1* homozygous KO mice. Bars indicate averages. Each circle represents the datum of a mouse.

index (WT, 7.70 ± 2.50; KO, 5.29 ± 1.16, d.f. = 18, $U = 42$, $P = 0.84$) and anticipatory activity index (WT, 0.14 ± 0.05; KO, 0.34 ± 0.21, d.f. = 18, $U = 41$, $P = 0.78$) did not differ between the KO mice and WT littermates (Fig. 1a–c).

There was no abnormality of free running period measured at the constant dark condition in *Wfs1* KO mice (average 23.7 h, $n = 6$). None of female KO mice showed significant periodicity in wheel-running activity with the duration of 4–5 days (data not shown). These results show that the behavioral phenotypes of *Wfs1* KO mice are different from the mPolg Tg mice that exhibit altered circadian rhythm of wheel-running activity (Kasahara et al., 2006).

3.2. Behavioral analysis: phase I. Screening by a test battery

To screen the behavioral abnormality of *Wfs1* KO mice, we performed a conventional behavioral test battery using 14 homozygous KO mice, 14 heterozygous KO mice, and 13 WT littermates. The results of behavioral tests are summarized in Table 1.

3.2.1. Open-field test

Although a significant effect of time was found for both locomotor activity (d.f. = 8.6, $F = 3.0$, $P = 0.002$) and rearing (d.f. = 11.0, $F = 9.7$, $P = 0.000$), no significant effect of genotype was found for locomotor activity (d.f. = 2, $F = 0.70$, $P = 0.49$) and rearing (d.f. = 2, $F = 0.57$, $P = 0.56$). There was no significant interaction between time and genotype (locomotor, d.f. = 17.3, $F = 21.1$, $P = 0.57$; rearing, d.f. = 22.0, $F = 0.80$, $P = 0.71$) (Fig. 2a and b).

3.2.2. Startle response and prepulse inhibition

When RMANOVA was applied for the data of startle response, significant effect of blocks was found (d.f. = 5.12, $F = 7.80$, $P < 0.001$). However, no significant effect of genotype (d.f. = 2, $F = 0.664$, $P = 0.52$) or genotype × block block interaction (d.f. = 10.2, $F = 1.30$, $P = 0.22$) was found (Fig. 2c). No significant effect of genotype was found for the PPI ratio regardless of the interval of prepulse (50 ms, d.f. = 2, $F = 0.38$, $P = 0.68$; 100 ms, d.f. = 2, $F = 0.65$, $P = 0.52$; 200 ms, d.f. = 2, $F = 0.41$, $P = 0.66$, one-way ANOVA) (Fig. 2d).

3.2.3. Elevated plus maze

The number of entry into the open arms ($F = 0.31$, d.f. = 2, $P = 0.72$, one-way ANOVA) (Fig. 2e) and the time spent in the open arms ($F = 2.05$, d.f. = 2, $P = 0.14$) (Fig. 2f) were not significantly different among the genotypes. A significant effect of genotype was found for the total number of boluses ($F = 7.16$, d.f. = 2, $P = 0.002$) (Fig. 2g). The Tukey honest significant difference (HSD) test showed that homozygous KO mice had a significantly lower number of fecal boluses (2.7 ± 0.3 [mean ± S.E.M.]) compared with heterozygous KO mice (4.8 ± 0.5, $P = 0.01$) and WT mice (5.2 ± 0.5, $P = 0.004$).

Table 1
Summary of findings in behavioral tests

Test battery	Findings
Wheel-running activity (34 weeks, 11 KO, 9 WT)	
Periodicity	NS
Diurnal activity rhythm	NS
Phase I (12 weeks, 13 KO, 14 Hetero, 13 WT)	
Open field	NS
Startle/PPI	NS
Elevated plus maze	NS
Morris water maze	NS
Passive avoidance test	Longer latency to move
Active avoidance test	Reduced number of escape at day 3
Forced swimming test	Reduced immobility on the second day
Phase II (31 weeks, 9 KO, 11 WT)	
Home cage activity	NS
Open field	NS
Light-dark box	NS
Elevated plus maze	NS
Startle/PPI	NS
Morris water maze	Increased escape latency without the change of distance traveled
Fear conditioning	Enhanced freezing during conditioning and before the cue at the cue test
Phase III (9 weeks, 7 KO, 8 WT)	
Social interaction	Decreased interaction
Rota-rod	NS
Sucrose preference	NS
Tail suspension test	NS
Forced swimming test	Reduced immobility on the second day
Marble burying test	NS
Hot plate test	NS
Tail flick test	NS

KO, *Wfs1* (−/−); Hetero, *Wfs1* (−/+); WT, *Wfs1* (+/+). PPI: prepulse inhibition test, NS, non-significant.

3.2.4. Morris water maze

The time to reach the platform during the 5-day learning phase became shorter than the first day, shown by a significant effect of day by RMANOVA (d.f. = 4, $F = 19.1$, $P < 0.001$) (Fig. 2h). However, there was neither significant effect of genotype (d.f. = 2, $F = 0.56$, $P = 0.57$) nor significant interaction of day and genotype (d.f. = 2, $F = 0.53$, $P = 0.94$). The time spent in the target quadrant (d.f. = 2, $F = 0.10$, $P = 0.90$, one-way ANOVA) and immobility time (d.f. = 2, $F = 0.58$, $P = 0.56$) at the probe test performed on day 6 did not show a significant difference among the genotypes (Fig. 2i).

3.2.5. Passive avoidance test

The latency to escape at the conditioning phase was significantly different among the genotypes (d.f. = 2, $F = 4.70$, $P = 0.015$, one-way ANOVA). Multiple comparison showed that the latency in homozygous KO mice was significantly longer than that in WT mice ($P = 0.02$) (Fig. 3a). There was no significant difference in escape latency at the test session (d.f. = 2, $F = 0.81$, $P = 0.92$, one-way ANOVA).

3.2.6. Active avoidance test

The time course of mean escape latency was examined during 3-days' training, consisting of 5 blocks in each day

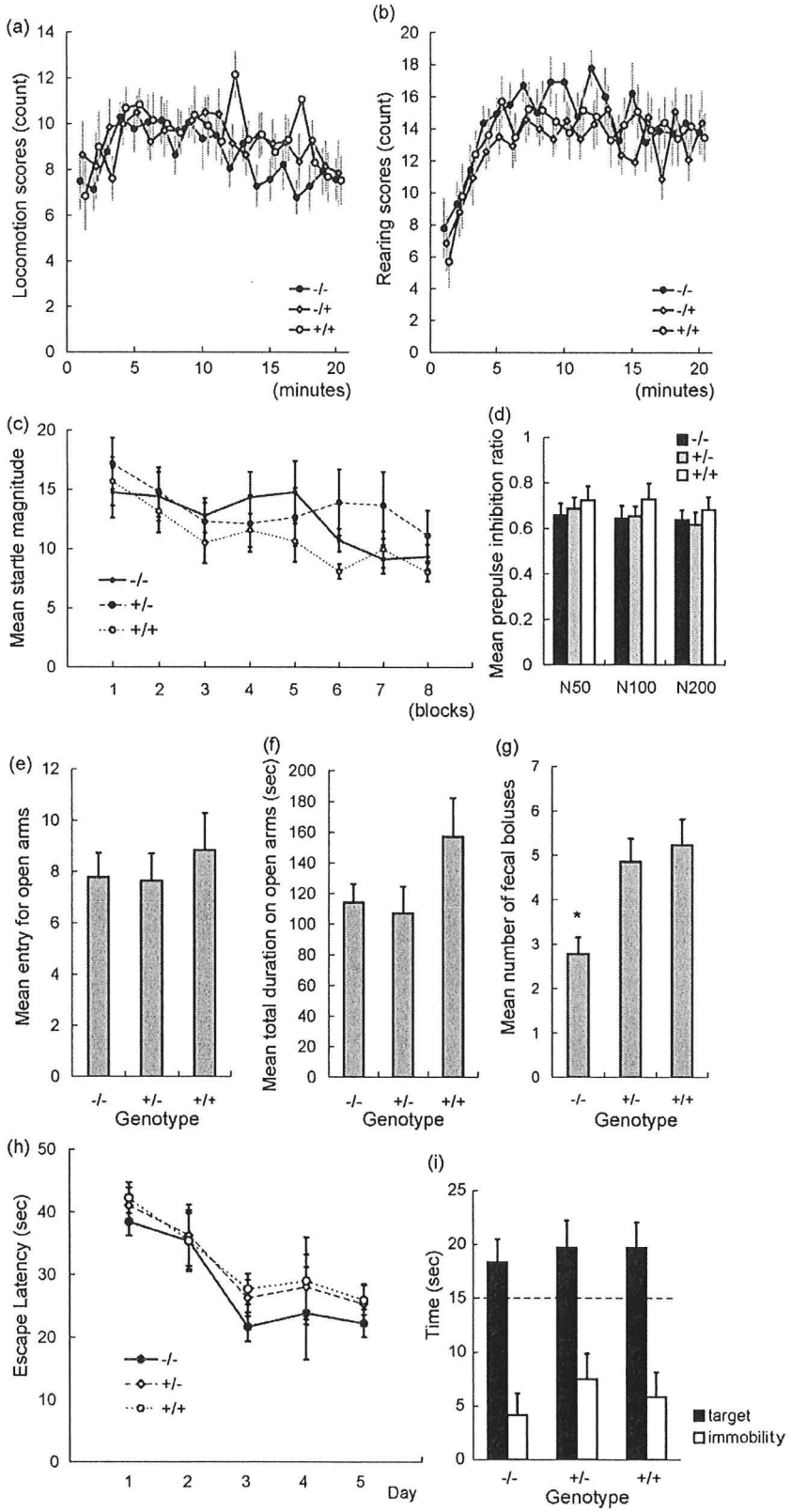

Fig. 2. Behavioral screening (1). (a–b) Open-field test. Locomotion scores (a) and rearing scores (b). Bars indicate the standard errors. (c) Startle response. (d) Prepulse inhibition test. N50 means the prepulse 50 ms before the startle pulse. (e–g) Elevated plus maze test. (h–i) Morris water maze test. Time course of escape latency during 5-days training (h), and time spent in the target quadrant during the 60-s session. Error bars represent standard error of mean. The dotted line represents the chance level. +/+, WT mice; +/−, *Wfs1* heterozygous KO mice; −/−, *Wfs1* homozygous KO mice. $^{*}P < 0.05$.

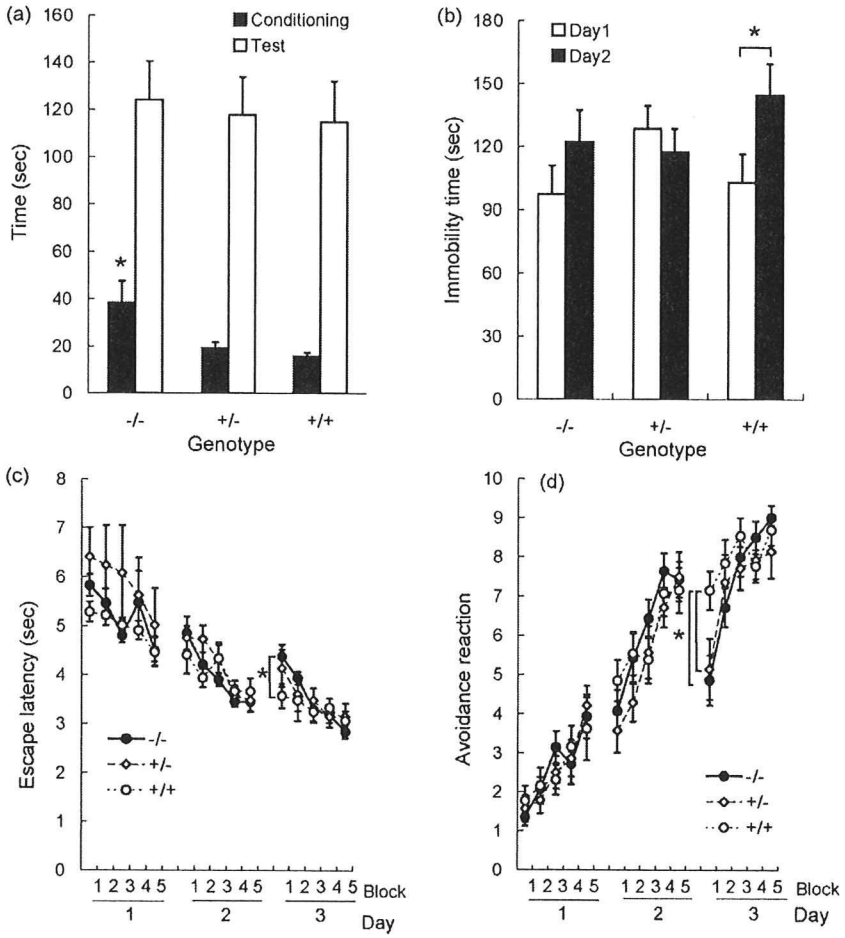

Fig. 3. Behavioral screening (2). (a) Passive avoidance test. (b) Forced swimming test performed on two sequential days. (c–d) Active avoidance test. +/+, WT mice; +/−, *Wfs1* heterozygous KO mice; −/−, *Wfs1* homozygous KO mice. Error bars represent standard error of mean. $^{*}P < 0.05$.

(Fig. 3c). In the three-way RMANOVA with the within-group factors of day and block and the between-group factor of genotype, although no significant effect of genotype was found (d.f. = 2, $F = 0.75$, $P = 0.47$), there was a significant interaction between genotype and block (d.f. = 1.75, $F = 2.94$, $P = 0.007$). No other two-way or three-way interactions were statistically significant. This significant interaction may be caused by longer escape latency of KO mice only at the first block. A post hoc analysis showed that the escape latency of the homozygous KO mice at the first block on day 3 was significantly longer than that in WT mice (d.f. = 25, $t = 2.34$, $P = 0.027$, with no correction for multiple comparison).

Similar interaction between genotype and block was also seen for the numbers of avoidance (d.f. = 6.3, $F = 3.25$, $P = 0.004$) (Fig. 3d). Both homozygous and heterozygous KO mice showed significantly lower numbers of avoidance at the first block on day 3 (homozygotes, d.f. = 25, $t = -2.82$, $P = 0.009$; heterozygotes, d.f. = 25, $t = -2.15$, $P = 0.04$).

3.2.7. *Forced swimming test*

When the immobility time was analyzed by RMANOVA, a significant effect of day (d.f. = 1, $F = 5.5$, $P = 0.024$) and a significant interaction of day and genotype (d.f. = 2, $F = 3.8$, $P = 0.031$) were found, whereas no significant effect of genotype was found (d.f. = 2, $F = 0.48$, $P = 0.61$) (Fig. 3b).

In the WT mice, immobility time was significantly longer on the second day (144.6 ± 53.0 s) compared with the first day (103.0 ± 48.3 s, d.f. = 12, $t = -3.45$, $P = 0.005$, paired t-test), possibly reflecting the learned despair (Parra et al., 1999). On the other hand, such a significant increase of immobility time on the second day was not observed for heterozygous (day 1, 128.5 ± 39.4 s; day 2, 117.5 ± 39.4 s; d.f. = 12, $t = 1.11$, $P = 0.28$) and homozygous (day 1, 97.4 ± 50.6 s; day 2, 122.0 ± 57.0 s; d.f. = 13, $t = -1.44$, $P = 0.17$) KO mice (Fig. 3b).

3.2.8. *Summary of the phase I behavioral analysis*

The results of the phase I behavioral analysis are summarized as follows.

(1) There was no abnormality in open field, elevated plus maze, PPI, and Morris water maze. However, it cannot be ruled out that the mice develop behavioral phenotypes at later age because depression is an adult-onset disease.
(2) The passive avoidance test showed the longer latency to enter the other chamber in *Wfs1* KO mice. This could be

explained either by low anxiety or retardation, that is slow movement or delayed onset of motion. However, it is also possible that mice could have been just busy exploring the first box, or they had some kind of place neophobia.

(3) The active avoidance test showed longer escape latency and lower numbers of avoidance at the first block on day 3 in *Wfs1* KO mice. This might suggest that the emotional memory is impaired in the *Wfs1* KO mice. It cannot be excluded, however, that *Wfs1* KO mice have impairment of pain sensitivity.

(4) Altered response to serial forced swimming test. This may suggest that the *Wfs1* KO mice tend to be resistant to behavioral despair.

3.3. Behavioral analysis: phase II

To further characterize the behavioral phenotypes of *Wfs1* KO mice, additional behavioral analysis was performed.

3.3.1. Open-field, elevated plus maze, PPI tests, and Morris Water Maze at 31 weeks

At first, four of behavioral tests were repeated in the mice aged 31 weeks to assess the effect of age. There were no significant difference between WT mice and *Wfs1* KO mice for three of these behavioral tests: open-field, elevated plus maze, and PPI tests (data not shown).

On the other hand, the Morris water maze test showed longer escape latency. Two-way RMANOVA showed significant effects of genotype (d.f. = 1, $F = 9.04$, $P = 0.008$) and day (d.f. = 3, $F = 8.45$, $P < 0.001$) (Fig. 4a). The *Wfs1* KO mice showed longer escape latency than controls. There was no significant interaction between genotype and day (d.f. = 3, $F = 0.60$, $P = 0.61$). On the other hand, there was no significant effect of genotype on the distance (d.f. = 1, $F = 0.38$, $P = 0.54$) (Supplementary Fig. 1a). Effect of day was significant (d.f. = 3, $F = 25.2$, $P < 0.001$), but the interaction between genotype and day was not significant (d.f. = 3, $F = 0.71$, $P = 0.54$). To assess the speed of swimming, a new index, swimming speed index = (total distance)/(latency to reach platform) was calculated. Two-way RMANOVA showed no significant effects of day (d.f. = 1.77, $F = 2.57$, $P = 0.09$) and genotype (d.f. = 1, $F = 0.04$, $P = 0.83$). There was no significant day × genotype interaction (d.f. = 1.77, $F = 0.33$, $P = 0.69$) (Supplementary Fig. 1b). Spatial memory cannot be assessed because no significant difference was found between the time spent in the target quadrant and that in the other three quadrants, suggesting that the probe test did not work properly even for wild-type mice (data not shown).

3.3.2. Home cage activity

To assess the general activity level, home cage activity was recorded for 8 days. When RMANOVA was applied, a significant effect of day (d.f. = 5, $F = 5.95$, $P < 0.001$) was found. There was no significant effect of genotype (d.f. = 1, $F = 0.61$, $P = 0.44$) and genotype × day interaction (d.f. = 5, $F = 0.53$, $P = 0.75$) (Fig. 4b).

3.3.3. Anxiety-like behavior

Next, the level of anxiety-like behavior was further assessed by the L-D box. The marble burying test was also performed in the 9-week-old mice in the phase III behavioral analysis.

In the L-D box test, no significant difference was found in the time spent in the light box (WT, 39.2 ± 9.0%, KO, 37.1 ± 9.8%, d.f. = 18, $t = 0.50$, $P = 0.61$). There was no significant difference in the number of marbles buried (WT 16.0 ± 0.8, KO 17.1 ± 0.7, $t = 1.0$, $P = 0.33$). These findings suggest that longer latency to escape at the passive avoidance test was not due to lower anxiety-like behavior.

3.3.4. Emotional memory

To test the hypothesis that emotional memory is impaired in the *Wfs1* KO mice, the fear conditioning test was performed.

During the conditioning phase, two-way RMANOVA revealed significant effect of genotype (d.f. = 1, $F = 4.47$, $P = 0.049$) and time (d.f. = 3.54, $F = 22.1$, $P < 0.001$). No significant period × genotype interaction was found (d.f. = 3.54, $F = 1.73$, $P = 0.16$). The *Wfs1* KO mice showed significantly longer time of freezing during the conditional stimuli (periods 5 and 7) and at the final period (Student's *t*-test, $P < 0.05$) (Fig. 4c).

For the cue test, two-way RMANOVA was applied to the data set before and after the cue, separately. For the data of freezing before the cue, a slight tendency of the effect of genotype (d.f. = 1, $F = 2.9$, $P = 0.10$) was seen, whereas there was significant effect of time (d.f. = 3, $F = 5.93$, $P = 0.001$) and no interaction between genotype and time (d.f. = 3, $F = 0.30$, $P = 0.82$). The *Wfs1* KO mice spent a significantly longer time for freezing ($t = 2.48$, $P < 0.01$) (Fig. 4d). However, no significant effect of genotype was found after the cue (effect of genotype, d.f. = 1, $F = 1.48$, $P = 0.23$; effect of time, d.f. = 3, $F = 1.60$, $P = 0.19$; genotype × time interaction, d.f. = 3, $F = 0.40$, $P = 0.75$). There was no significant effect of genotype at the context test (Fig. 4e).

These findings suggested that memory of emotion is not impaired in the *Wfs1* KO mice.

3.4. Behavioral analysis: phase III

3.4.1. Pain sensation

As noted above, it cannot be excluded that *Wfs1* KO mice have impairment of pain sensitivity. To rule out such possibility, the hot plate test and tail flick test were performed. No difference in the latency to licking (WT, 10.3 ± 1.2 s; KO, 9.9 ± 0.9 s, $t = 0.219$, d.f. = 12, $P = 0.83$, by Student's *t*-test) was found between the *Wfs1* KO mice and WT mice by the hot plate test. There was no significant difference in the latency to flick the tail (WT, 3.5 ± 0.2 s; KO, 3.4 ± 0.2 s, d.f. = 12, $t = 0.29$, $P = 0.77$).

3.4.2. Motor function

As noted above, many of the positive findings in behavioral tests can be interpreted as reflecting retardation. Such findings can be explained by altered motor functions, such as impairment in muscle contraction, voluntary movement, or

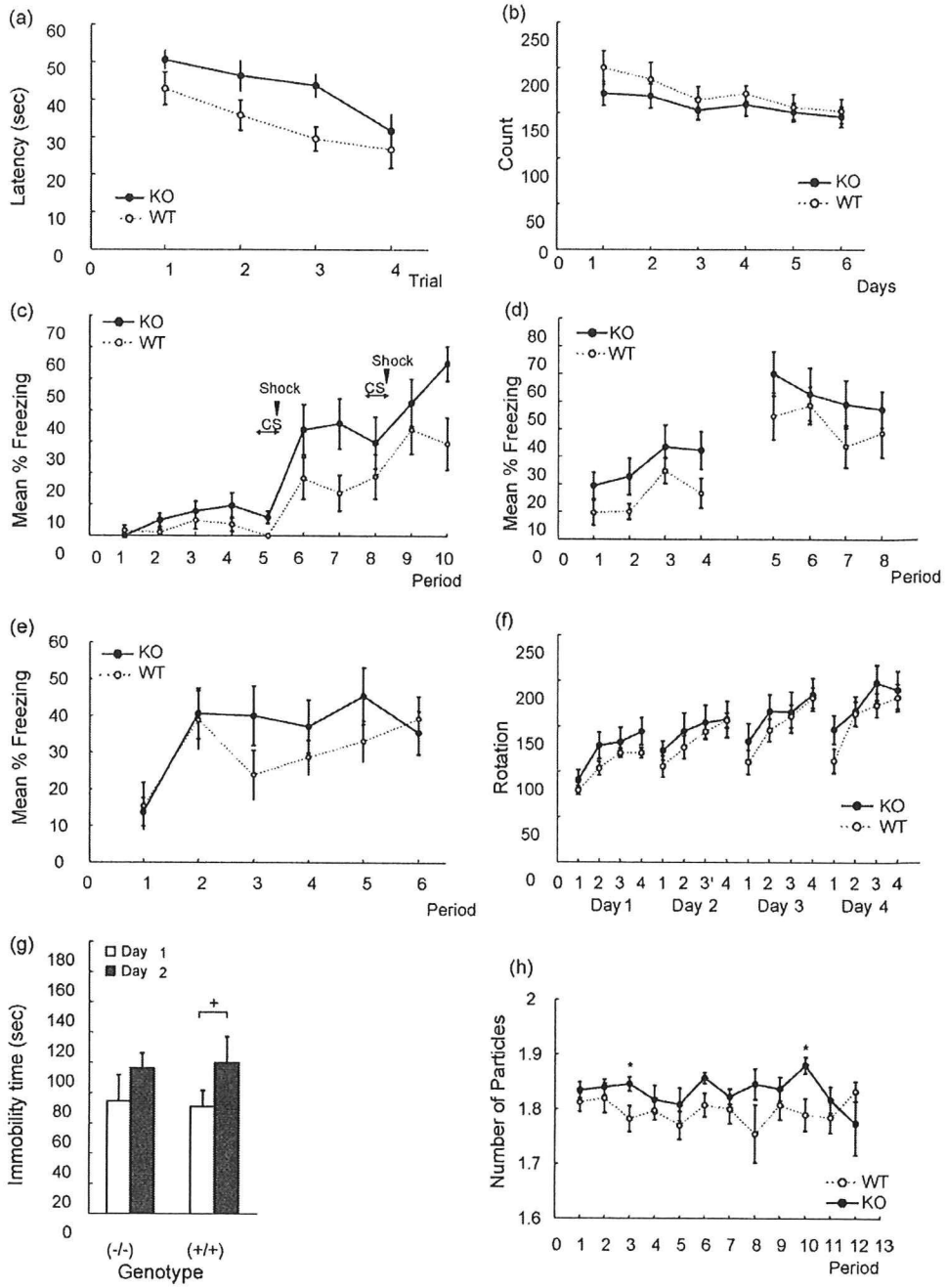

Fig. 4. Further characterization of behavioral phenotypes of *Wfs1* KO mice. (a) Morris water maze test. (b) Home cage activity. (c and d) Fear conditioning test. One time period is 30 s. (c) Conditioning phase. Conditional stimuli (tone) and unconditional stimuli (foot shock) were applied during periods 5 and 8. (d) Cue test. Cue was applied between the time periods 4 and 5. (e) Context test. (f) Rotarod test. (g) Forced swimming test. (h) Social interaction test. Note that high number of particles indicates lower levels of social interaction.

motor coordination. To test this possibility, the rotarod test was performed. Three-way RMANOVA with the intra-individual factors of day and trial and inter-individual factor of genotype showed no significant effect of genotype (d.f. = 1, $F = 1.02$, $P = 0.33$). Whereas significant effects of day (d.f. = 3, $F = 15.6$, $P < 0.001$) and trial (d.f. = 3, $F = 51.0$, $P < 0.001$) were found, no significant two-way or three-way interactions were detected except for a trend of interaction between day and trial (d.f. = 3, $F = 2.54$, $P = 0.07$) (Fig. 4f).

3.4.3. Behavioral despair

As noted above, *Wfs1* KO mice showed altered response to the serial forced swimming test. To further confirm this finding, the forced swimming test was performed again.

RMANOVA revealed a tendency of effect of day (d.f. = 1.0, $F = 3.83$, $P = 0.07$). There was no significant effect of genotype (d.f. = 1, $F = 0.18$, $P = 0.67$) and day × genotype interaction (d.f. = 1.0, $F = 0.17$, $P = 0.68$).

Although no day × genotype interaction was found in this analysis, the paired *t*-test was applied similarly to the first experiment (Fig. 4g). Immobility time tended to be longer on the second day (99.7 ± 17.4 s) compared with the first day (71.0 ± 10.55 s, $r = 0.68$, $P = 0.064$, paired *t*-test) in WT mice, whereas no significant difference was found in *Wfs1* KO mice (day 1, 74.5 ± 17.1 s; day 2, 96.2 ± 10.0 s, $r = 0.50$, $P = 0.24$). This analysis showed a similar tendency to the first experiment.

The other test of behavioral despair, the tail suspension test, was also performed. There was no significant difference in the immobile time between the *Wfs1* KO mice and WT mice (WT, 9.0 ± 2.8%; KO, 9.4 ± 3.0%, $t = 0.09$, $P = 0.92$).

3.4.4. Other aspects of depression

Some of these noted findings in the *Wfs1* KO mice can be explained by the retardation in emotionally triggered motion. This could not be explained by abnormalities in instrumental motor functions. Such findings seem to be similar to "psychomotor retardation" seen in human depressive patients. Though the findings in the forced swimming test and tail suspension test are equivocal, behavioral despair is not always a valid depression model. Thus, we further examined the other aspects of depression.

The sucrose preference test is an established test for anhedonia, one of the core symptoms of depression. In the choice test for 3 days, there was no significant effect of genotype (d.f. = 1, $F = 0.95$, $P = 0.34$) by two-way RMANOVA (WT, day 1, 44.2 ± 16.7%, day 2, 94.1 ± 5.2%, day 3, 84.5 ± 9.7%; KO, day 1, 37.3 ± 12.9%, day 2, 97.3 ± 1.7%, day 3, 60.2 ± 16.0%). A significant effect of trial (d.f. = 2, $F = 10.7$, $P = 0.001$) and no significant interaction of genotype × trial was found (d.f. = 2, $F = 0.68$, $P = 0.51$). The 1-h choice test after 24-h water deprivation did not show a significant difference between genotypes (WT 90.2 ± 1.7%, KO 86.3 ± 5.3%, $U = 28$, NS).

The social interaction test is an established test for anxiety-like behavior (File and Seth, 2003). However, its response to drugs is different from elevated plus maze, and it is more sensitive to serotonergic drugs. Recently, this test is also applied to animal models of schizophrenia (Miyakawa et al., 2003) and autism, and to genetic models of anxiety and depression (Overstreet et al., 2003). Thus, social behavior of the *Wfs1* KO mice was examined by this test. Two-way RMANOVA revealed no significant effect of genotype (d.f. = 1, $F = 2.0$, $P = 0.17$) and time (d.f. = 11, $F = 0.93$, $P = 0.51$). There was a trend of genotype × time interaction (d.f. = 11, $F = 1.67$, $P = 0.08$) (Fig. 4h). The *Wfs1* KO mice showed significant decrease of social interaction at the periods 3 and 10 (Student's *t*-test, $P < 0.05$) shown by the higher number of particles observed.

3.5. Wfs1 immunohistochemistry

To determine the molecular basis of behavioral abnormality in *Wfs1* KO mice, we verified whether the distribution of *Wfs1* protein in the brains of WT B6 mice is similar to that in rats (Fig. 5a–f) (Takeda et al., 2001). We verified that no staining was observed in *Wfs1* KO mice, suggesting the specificity of the anti-*Wfs1* antibody (Fig. 5g).

Wfs1-like immunoreactivity (*Wfs1*-IR) localized mostly to neurons and its regional distribution was mostly similar to that in rats (Fig. 5a). *Wfs1*-IR was most abundant in the hippocampal CA1 pyramidal neurons (Fig. 5b), and strong in the layer II pyramidal neurons of the cerebral cortex (Fig. 5c). Similar to rats, *Wsf1*-IR was also rich in the striatum, nucleus accumbens, thalamus, cerebellar Purkinje cells, amygdala, and bed nucleus of the stria terminalis (Fig. 5d). In addition, *Wfs1*-IR was observed in several hypothalamic nuclei, such as the paraventricular nucleus and suprachiasmatic nucleus (SCN) in mice (Fig. 5e). In the adjacent region of SCN, sub-paraventricular zone, some cell bodies showed *Wfs1*-IR. The ventromedial nucleus and arcuate nucleus also showed *Wfs1*-IR (Fig. 5f). *Wfs1*-IR was also found in the locus coeruleus and cochlea nucleus (data not shown).

3.6. DNA microarray analysis

To examine what sort of functional impairment occurs in the neurons of *Wfs1* KO mice, we performed gene expression analysis using DNA microarray. Because *Wfs1*-IR was most abundant in hippocampus, we performed DNA microarray analysis in the hippocampus of the *Wfs1* KO mice. A total of 1012 probe sets were changed at the age of 12 weeks. To narrow down the gene list, we repeated the experiment at the age of 30 weeks. We assumed that the true gene expression difference observed at age 12 weeks should be replicated at age 30 weeks. At the age of 30 weeks, 3508 probe sets showed significant differences. The genes altered in the same direction at both the ages of 12 and 30 weeks, and the fold change higher than 1.2 are shown in Table 2.

GeneOntology (GO) analysis showed that genes related to ribosome biogenesis (GO:3735: structural constituent of ribosome, GO:7046: ribosome biogenesis, GO:3723: RNA binding) or other basic cellular functions (GO:5622: intracellular, GO:44249: cellular biosynthesis, GO:15399: primary active transporter activity, GO:5623: cell, GO:7028: cytoplasm organization and biogenesis) were commonly up-regulated at the age of 12 and 30 weeks (Supplementary Tables 1 and 2). The major difference between the weeks 12 and 30 is the inclusion of neurodevelopment-related genes at the age of 30 weeks (GO:48666: neuron development, GO:30182: neuron differentiation, GO:7409: axonogenesis, GO:48667: neuron morphogenesis during differentiation, and GO:31175: neurite morphogenesis) (Supplementary Table 2).

3.7. RT-PCR analysis

To test whether the findings by DNA microarray analysis are chance findings, RT-PCR analysis was performed. For this purpose, two down-regulated genes, *cdc42ep5* and *Rnd1*, as well as two up-regulated genes, *Wnt2* and *Garnl1*, were examined using Gapdh as a reference.

The level of cdc42ep5 and Rnd1 tended to be lower at 12 weeks but not at 32 weeks. On the other hand, Wnt2 and Garnl1

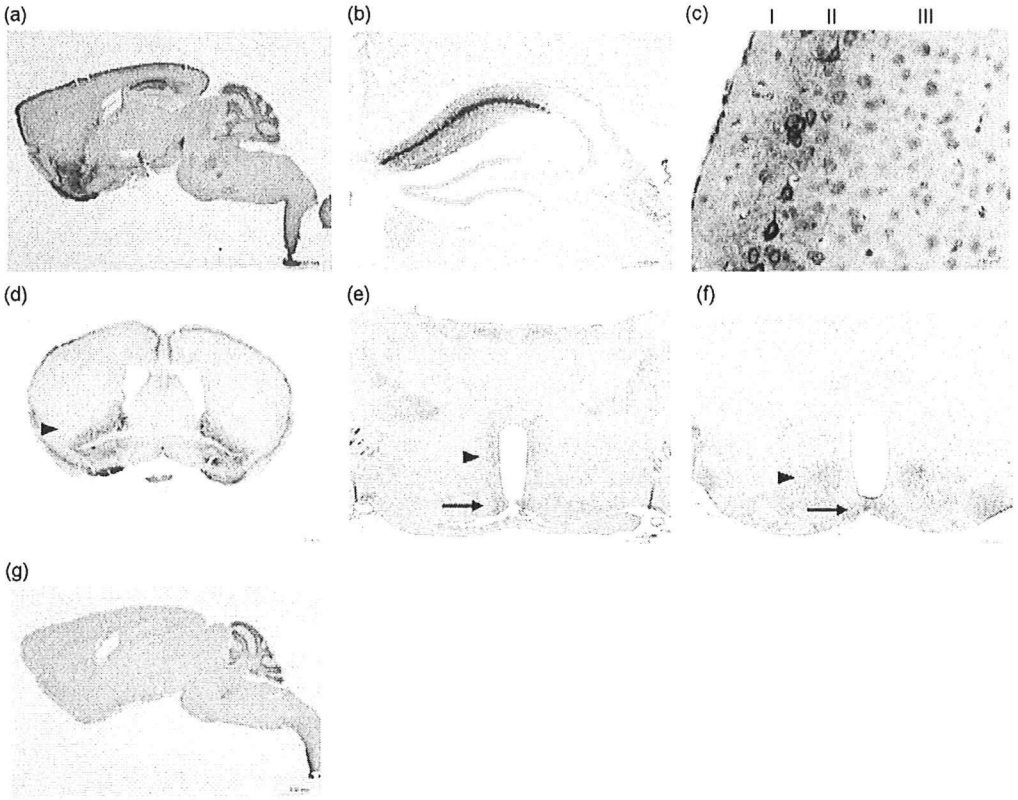

Fig. 5. Localization of *Wfs1*-like immunoreactivity in mouse brain. Immunohistochemistry analysis of mouse brain using anti-*Wfs1* antiserum. Coronal sections are shown except for panel a. (a) Sagittal section of the whole brain. (b) Hippocampus. CA1 (corpus ammon 1) region is selectively stained. (c) Cerebral cortex. Layer II pyramidal neurons are stained. (d) Coronal section at the level of bed nucleus of striata terminalis (BNST). At this level, the regions with intense *Wfs1*-IR looked as if they are surrounding the internal capsule (arrowhead). (e and f) Hypothalamus. Suprachiasmatic nucleus and sub-paraventricular zone are indicated by an arrow and an arrowhead, respectively (e). Arcuate nucleus and ventromedial nucleus are shown by an arrow and an arrowhead, respectively (f). (g) Immunohistochemistry analysis of the brain of a *Wfs1* KO mouse using anti-*Wfs1* antiserum. No staining is detected.

were significantly up-regulated at 32 weeks but not at 12 weeks (Table 3).

4. Discussion

4.1. Behavioral analyses

We recently reported that mPolg Tg mice show bipolar disorder-like behavioral phenotypes, such as altered circadian rhythm in both males and females and periodic fluctuation of wheel-running activity in females (Kasahara et al., 2006). Based on previous reports suggesting that patients with Wolfram disease are frequently affected with depression or bipolar disorder, we speculated that the *Wfs1* KO mice might also show these bipolar disorder-like phenotypes, which were seen in the mPolg Tg mice. However, *Wfs1* KO mice did not show similar phenotypes (Fig. 1).

Thus, we next examined the possibility that *Wfs1* KO mice show other types of behavioral phenotypes. At first, a battery of established behavioral tests was applied. There was no marked difference found in most of conventional behavioral tests, such as the open-field test, startle response, prepulse inhibition test, and elevated plus maze. The lack of marked difference in these tests was replicated in the mice aged 31 weeks. On the other hand, several tests in the initial test battery showed equivocal findings. In the passive avoidance test, the mice showed longer latency to move into the dark compartment at the training phase (Fig. 3a). The active avoidance test showed subtle differences between the KO and WT mice. On the third day of training, WT mice kept the same level of escape latency and number of avoidance reactions as the final block of the second day. Although, *Wfs1* KO mice seemed as if they forget the previous memory of escape training (Fig. 3c and d), it is unlikely considering the fact that there were no differences in the day 2 of the active avoidance test and in the contextual testing of the fear conditioning test. Otherwise, they may remember the events, but could not take the adequate action under the situation for some other reasons. For example, a possibility is that they showed retardation or increased behavioral despair without any problems in memory retention. In the forced swimming test performed for two sequential days, WT mice showed an increase of immobility time on the second day (Fig. 3d). This is in accordance with a previous study showing that mice became immobile on the second day of the sequential forced swimming test (Parra et al., 1999). This phenomenon was not observed in the homozygous and heterozygous KO mice (Fig. 3d). Although statistical analysis did not show the same difference, a similar tendency was observed in the second

Table 2
Probe sets commonly altered both at 12 and 30 weeks

Probe set ID	*P*-value		Fold change		Gene symbol	chromosome	Gene title
	12W	30W	12W	30W			
Down							
1433815 at	0.0008	0.0074	−2.24	−1.72	Jakmip1	5qB3[a]	Janus kinase and microtubule interacting protein 1
1448411 at	0.0008	0.0045	−2.10	−2.00	*Wfs1*	5qB3[a]	Wolfram syndrome 1
1419744 at	0.0357	0.0424	−1.45	−1.44	H2-DMb2	17qB1	Histocompatibility 2, class II, locus Mb2
1442241 at	0.0357	0.0424	−1.41	−1.49	Srpk2	5qA3[a]	Serine/arginine-rich protein specific kinase 2
1425620 at	0.0157	0.0284	−1.39	−1.22	Tgfbr3	5qE5[a]	Transforming growth factor, beta receptor III
1418712 at	0.0274	0.0284	−1.36	−1.47	Cdc42ep5	7qA1	CDC42 effector protein (Rho GTPase binding) 5
1441317 x at	0.0011	0.0045	−1.34	−1.71	Jakmip1	5qB3[a]	Janus kinase and microtubule interacting protein 1
1455197 at	0.0357	0.0424	−1.26	−1.29	Rnd1	15qF1	Rho family GTPase 1
Up							
1418148 at	0.0087	0.0074	2.03	1.68	Abhd1	5qB1[a]	Abhydrolase domain containing 1
1431328 at	0.0046	0.0424	1.50	1.21	Ppp1cb	5qB1[a]	Protein phosphatase 1, catalytic subunit, beta isoform
1459714 at	0.0157	0.0284	1.35	1.57	–	4qE1	–
1449425 at	0.0357	0.0074	1.28	1.28	Wnt2	6qA2	Wingless-related MMTV integration site 2
1457532 at	0.0357	0.0185	1.27	1.35	Garnli	12qC1	GTPase activating RANGAP domain-like 1
1416569 at	0.0274	0.0118	1.25	1.24	Actl6a	3qA3	Actin-like 6A
1446406 at	0.0460	0.0424	1.24	1.20	Paqr8	1qA4	Progestin and adipoQ receptor family member VIII
1446815 at	0.0357	0.0424	1.23	1.29	Dph4	2qE3	DPH4 homolog (JJJ3, S. cerevisiae)
1456328 at	0.0460	0.0284	1.22	1.33	Bank1	3qG3	B-cell scaffold protein with ankyrin repeats 1

[a]The probe sets on the chromosome 5.

forced swimming test. In addition, the other test for behavioral despair, the tail suspension test, did not show any significant difference. On the other hand, the longer escape latency of the KO mice without the difference of the distance traveled in the Morris water maze might reflect the longer time for immobility during the session. Thus, the *Wfs1* KO mice might show enhanced or attenuated behavioral despair depending on experimental conditions.

Table 3
Validation study of gene expression using RT-PCR

Gene	Genotype	N	Average	S.E.M.	*P*-value
12w					
cdc42ep5	WT	8	0.68	0.02	
	KO	8	0.63	0.02	0.088*
Rnd1	WT	8	0.42	0.01	
	KO	8	0.39	0.02	0.070*
Wnt2	WT	8	0.42	0.01	
	KO	8	0.44	0.02	0.227
Garnl1	WT	8	15.30	0.37	
	KO	8	14.62	0.61	0.180
32w					
cdc42ep5	WT	5	0.63	0.01	
	KO	7	0.66	0.03	0.225
Rnd1	WT	5	0.58	0.04	
	KO	7	0.54	0.04	0.235
Wnt2	WT	5	0.40	0.01	
	KO	7	0.44	0.02	0.041**
Garnl1	WT	5	12.95	0.16	
	KO	7	14.37	0.64	0.049**

The gene expression levels were normalized by Gapdh. Each value represents the gene/Gapdh ratio × 10^{-2}. *P*-values were calculated by Mann–Whitney *U*-test (one tailed).
* $P < 0.10$
** $P < 0.05$.

As described above, it was speculated that longer latency to move at the passive avoidance test can be explained either by low anxiety or retardation of *Wfs1* KO mice. The former possibility was not supported by two established tests for anxiety-like behavior, the L-D box test, and the marble burying test.

Wfs1 KO mice also showed longer escape latency and lower numbers of avoidance during the active avoidance test. This was not due to decreased pain sensitivity. This cannot be explained by the impairment of emotional memory, because there was no significant abnormality in fear conditioning test. This test instead showed increased freezing during conditioning phase. Freezing was also increased during the cue test, not after the cue but before the cue.

The *Wfs1* KO mice did not show impairment in fundamental motor functions that can explain these findings.

In summary, the following findings were obtained.

(1) Longer latency to move in passive avoidance test.
(2) Diminished avoidance reaction during active avoidance test.
(3) Longer escape latency in Morris water maze.
(4) Increased freezing during conditioning.
(5) Normal sensorimotor function and anxiety-like behavior.

These findings together suggest that the *Wfs1* KO mice might show retardation in the emotionally triggered motion. We could not discriminate whether this feature of the *Wfs1* KO mice reflects the slow movement, longer time to initiate movement, or mixture of both. Psychomotor retardation, that is, slow voluntary movement and thoughts and/or taking longer

time to initiate movement, is one of the characteristic symptoms of melancholic depression. The observed retardation of the *Wfs1* KO mice resembled such a characteristic symptom of depression. Thus, other aspects of depression were also examined. Although, the sucrose preference test did not show any difference, the social interaction test showed decreased social interaction in *Wfs1* KO mice.

Together these results suggest that *Wfs1* KO mice have some similarity to patients with depressive disorder. It should be noted, however, that the observed difference in the social interaction test might also reflect the retardation noted above. The *Wfs1* KO mice did not show marked abnormalities in the conventional behavioral despair paradigm, such as the forced swimming test and tail suspension test. These tests are established as screening tests for compounds having tricyclic antidepressant-like properties. However, its construct validity as a depression model is questioned (Crawley, 2007).

Taken together, the *Wfs1* KO mice show behavioral alterations at least partly mimicking the symptoms of depression. Further studies to examine the effects of antidepressive agents would be extremely interesting.

4.2. Morphologic analyses

Immunohistochemistry demonstrated that the distribution of *Wfs1*-IR was similar to that in rats (Fig. 5) (Takeda et al., 2001). In addition, we found that *Wfs1*-IR is also present in the hypothalamus. The presence of *Wfs1*-IR in the arcuate nucleus seems to be in accordance with diabetes insipidus, the major symptom of Wolfram disease. In a similar way, *Wfs1*-IR in the cochlea nucleus may be relevant to deafness in patients with Wolfram disease. It is also interesting that *Wfs1*-IR is found in the locus coeruleus and substantia nigra, from which noradrenergic and dopaminergic fibers originate. In *Wfs1* KO mice, however, we did not observe marked morphologic alterations in these regions using hematoxylin–eosin staining and Kluver-Barrera staining (data not shown).

4.3. Gene expression analysis

The fact that *Wfs1* itself is included in the list of altered genes (Table 2) supports the validity of our experiment and data analysis. Among the eight down-regulated and nine up-regulated genes, six other genes in addition to *Wfs1* itself were on the chromosome 5. This is possibly caused by residual genomic region derived from the 129Sv mice. Thus, only a part of these changes can be attributable to the absence of *Wfs1* itself. The present result is in accordance with a previous report that there were only small differences in expression profiles seen in fibroblasts obtained from patients with Wolfram disease (Philbrook et al., 2005).

Among the three down-regulated genes outside chromosome 5, two (*Cdc42ep5* and *Rnd1*) were related to Rho GTPase. Down-regulation of Rnd1 was validated at the age of 12 weeks but not at 32 weeks.

Cdc42ep5 encodes CDC42 effector protein. CDC42 plays a role in dendrite development (Threadgill et al., 1997). *Cdc42ep5* is one of the targets of CDC42 (Joberty et al., 1999), but its function in neurons is not known yet. *Rnd1* also plays a role in activity-dependent dendrite development (Ishikawa et al., 2006). A recent fine mapping analysis of 13q33 in bipolar disorder revealed the linkage with DOCK9, an activator of Cdc42 (Detera-Wadleigh et al., 2007). This finding also suggested the possible role of Rho GTPase in mood disorder. Together with the GO analysis showing altered neural development related genes at age 30 weeks, these findings may suggest that dendrite development may be impaired in *Wfs1* KO mice. Although, we did not observe morphologic difference between *Wfs1* KO mice and WT littermates using hematoxylin–eosin staining and Kluver-Barrera staining, dendrite morphology cannot be assessed using these methods. Further analysis by Golgi staining or other methods might be promising.

Up-regulation of two genes were validated at 32 weeks but not at 12 weeks. Up-regulation of Wnt2 is potentially interesting because Wnt signaling plays a role in neural plasticity and is implicated in the molecular pathology of bipolar disorder (Gould and Manji, 2002; Matigian et al., 2007).

Up-regulation of ribosome-related genes at both 12 and 30 weeks revealed by gene ontology analysis might be in accordance with the putative role of *WfS1* in ER stress response (Fonseca et al., 2005; Yamada et al., 2006).

4.4. Phenotypic discordance between Wfs1 KO mice and patients with Wolfram disease

In this study, *Wfs1* KO mice did not show marked sensorimotor and general health problems that are seen in patients with Wolfram disease. This is in accordance with the lack of spontaneous diabetes mellitus in *Wfs1* KO mice on the B6 background (Ishihara et al., 2004). Although, we detected some behavioral phenotypes in KO mice, it cannot be ruled out that some of detected behavioral alterations in *Wfs1* KO mice could be explained by the residual genomic region derived from 129Sv mice (Mouse Phenome Database, http://phenome.jax.org/pub-cgi/phenome/mpdcgi?rtn=docs/home).

It is possible that the symptoms in patients with Wolfram disease are the combination of the loss of function of *WfS1* and the dominant-negative effect of the mutations. Meta-analysis of genotype–phenotype correlation in Wolfram disease suggested that nonsense or frame-shift mutations caused more severe phenotypes compared with missense mutations (Cano et al., 2007). The *Wfs1* KO mice we analyzed in this study are *Wfs1*-null mice. On the other hand, another line of *Wfs1* KO mice, in which the exon 8 of *Wfs1* is deficient, was reported to show striking behavioral phenotypes (European Patent EP1353549). These findings suggest the possibility that the symptoms of Wolfram disease are accelerated by the aberrant proteins truncated around exon 8. Because function of *Wfs1* has not been well established yet, it is difficult to conclude which mechanism, loss of function or dominant-negative effect, is more influential. Further studies will be necessary to make draw a conclusion.

In summary, we studied the behavior and gene expression patterns in *Wfs1*-null mice. The *Wfs1* KO mice showed several

behavioral features, such as retardation in emotionally triggered motion, decreased social interaction, and enhanced or attenuated behavioral despair depending on experimental conditions. These findings might be relevant to the neuropsychiatric phenotypes reported in patients with Wolfram disease.

Appendix A. Supplementary data

Supplementary data associated with this article can be found, in the online version, at doi:10.1016/j.neures.2008.02.002.

References

Als, T.D., Dahl, H.A., Flint, T.J., Wang, A.G., Vang, M., Mors, O., Kruse, T.A., Ewald, H., 2004. Possible evidence for a common risk locus for bipolar affective disorder and schizophrenia on chromosome 4p16 in patients from the Faroe Islands. Mol. Psychiatry 9, 93–98.

Cano, A., Rouzier, C., Monnot, S., Chabrol, B., Conrath, J., Lecomte, P., Delobel, B., Boileau, P., Valero, R., Procaccio, V., Paquis-Flucklinger, V., Vialettes, B., 2007. Identification of novel mutations in WFS1 and genotype-phenotype correlation in Wolfram syndrome. Am. J. Med. Genet. A 143, 1605–1612.

Cheng, R., Juo, S.H., Loth, J.E., Nee, J., Iossifov, I., Blumenthal, R., Sharpe, L., Kanyas, K., Lerer, B., Lilliston, B., Smith, M., Trautman, K., Gilliam, T.C., Endicott, J., Baron, M., 2006. Genome-wide linkage scan in a large bipolar disorder sample from the National Institute of Mental Health genetics initiative suggests putative loci for bipolar disorder, psychosis, suicide, and panic disorder. Mol. Psychiatry 11, 252–260.

Crawford, J., Zielinski, M.A., Fisher, L.J., Sutherland, G.R., Goldney, R.D., 2002. Is there a relationship between Wolfram syndrome carrier status and suicide? Am. J. Med. Genet. 114, 343–346.

Crawley, J.N., 2007. What's Wrong with My Mouse? Behavioral Phenotyping of Transgenic and Knockout Mice. second ed. Wiley, Hoboken.

Detera-Wadleigh, S.D., Badner, J.A., Berrettini, W.H., Yoshikawa, T., Goldin, L.R., Turner, G., Rollins, D.Y., Moses, T., Sanders, A.R., Karkera, J.D., Esterling, L.E., Zeng, J., Ferraro, T.N., Guroff, J.J., Kazuba, D., Maxwell, M.E., Nurnberger Jr., J.I., Gershon, E.S., 1999. A high-density genome scan detects evidence for a bipolar-disorder susceptibility locus on 13q32 and other potential loci on 1q32 and 18p11.2. Proc. Natl. Acad. Sci. U.S.A. 96, 5604–5609.

Detera-Wadleigh, S.D., Liu, C.Y., Maheshwari, M., Cardona, I., Corona, W., Akula, N., Steele, C.J., Badner, J.A., Kundu, M., Kassem, L., Potash, J.B., Gibbs, R., Gershon, E.S., Mcmahon, F.J., 2007. Sequence variation in DOCK9 and heterogeneity in bipolar disorder. Psychiatry Genet. 17, 274–286.

Domenech, E., Gomez-Zaera, M., Nunes, V., 2006. Wolfram/DIDMOAD syndrome, a heterogenic and molecularly complex neurodegenerative disease. Pediatr. Endocrinol. Rev. 3, 249–257.

Evans, K.L., Lawson, D., Meitinger, T., Blackwood, D.H., Porteous, D.J., 2000. Mutational analysis of the Wolfram syndrome gene in two families with chromosome 4p-linked bipolar affective disorder. Am. J. Med. Genet. 96, 158–160.

Ewald, H., Degn, B., Mors, O., Kruse, T.A., 1998. Support for the possible locus on chromosome 4p16 for bipolar affective disorder. Mol. Psychiatry 3, 442–448.

Ewald, H., Flint, T., Kruse, T.A., Mors, O., 2002. A genome-wide scan shows significant linkage between bipolar disorder and chromosome 12q24.3 and suggestive linkage to chromosomes 1p22-21, 4p16, 6q14-22, 10q26 and 16p13. 3. Mol. Psychiatry 7, 734–744.

File, S.E., Seth, P., 2003. A review of 25 years of the social interaction test. Eur. J. Pharmacol. 463, 35–53.

Fonseca, S.G., Fukuma, M., Lipson, K.L., Nguyen, L.X., Allen, J.R., Oka, Y., Urano, F., 2005. WFS1 is a novel component of the unfolded protein response and maintains homeostasis of the endoplasmic reticulum in pancreatic beta-cells. J. Biol. Chem. 280, 39609–39615.

Gould, T.D., Manji, H.K., 2002. The Wnt signaling pathway in bipolar disorder. Neuroscientist 8, 497–511.

Inoue, H., Tanizawa, Y., Wasson, J., Behn, P., Kalidas, K., Bernal-Mizrachi, E., Mueckler, M., Marshall, H., Donis-Keller, H., Crock, P., Rogers, D., Mikuni, M., Kumashiro, H., Higashi, K., Sobue, G., Oka, Y., Permutt, M.A., 1998. A gene encoding a transmembrane protein is mutated in patients with diabetes mellitus and optic atrophy (Wolfram syndrome). Nat. Genet. 20, 143–148.

Ishihara, H., Takeda, S., Tamura, A., Takahashi, R., Yamaguchi, S., Takei, D., Yamada, T., Inoue, H., Soga, H., Katagiri, H., Tanizawa, Y., Oka, Y., 2004. Disruption of the WFS1 gene in mice causes progressive beta-cell loss and impaired stimulus-secretion coupling in insulin secretion. Hum. Mol. Genet. 13, 1159–1170.

Ishikawa, Y., Katoh, H., Negishi, M., 2006. Small GTPase Rnd1 is involved in neuronal activity-dependent dendritic development in hippocampal neurons. Neurosci. Lett. 400, 218–223.

Joberty, G., Perlungher, R.R., Macara, I.G., 1999. The Borgs, a new family of Cdc42 and TC10 GTPase-interacting proteins. Mol. Cell Biol. 19, 6585–6597.

Kakiuchi, C., Ishiwata, M., Hayashi, A., Kato, T., 2006. XBP1 induces WFS1 through an endoplasmic reticulum stress response element-like motif in SH-SY5Y cells. J. Neurochem. 97, 545–555.

Kasahara, T., Kubota, M., Miyauchi, T., Noda, Y., Mouri, A., Nabeshima, T., Kato, T., 2006. Mice with neuron-specific accumulation of mitochondrial DNA mutations show mood disorder-like phenotypes. Mol. Psychiatry 11, 577–593 523.

Kato, T., Kato, N., 2000. Mitochondrial dysfunction in bipolar disorder. Bipolar Disord. 2, 180–190.

Martorell, L., Zaera, M.G., Valero, J., Serrano, D., Figuera, L., Joven, J., Labad, A., Vilella, E., Nunes, V., 2003. The WFS1 (Wolfram syndrome 1) is not a major susceptibility gene for the development of psychiatric disorders. Psychiatry Genet. 13, 29–32.

Matigian, N., Windus, L., Smith, H., Filippich, C., Pantelis, C., Mcgrath, J., Mowry, B., Hayward, N., 2007. Expression profiling in monozygotic twins discordant for bipolar disorder reveals dysregulation of the WNT signalling pathway. Mol. Psychiatry 12, 815–825.

Miyakawa, T., Leiter, L.M., Gerber, D.J., Gainetdinov, R.R., Sotnikova, T.D., Zeng, H., Caron, M.G., Tonegawa, S., 2003. Conditional calcineurin knockout mice exhibit multiple abnormal behaviors related to schizophrenia. Proc. Natl. Acad. Sci. U.S.A. 100, 8987–8992.

Ohtsuki, T., Ishiguro, H., Yoshikawa, T., Arinami, T., 2000. WFS1 gene mutation search in depressive patients: detection of five missense polymorphisms but no association with depression or bipolar affective disorder. J. Affect Disord. 58, 11–17.

Osman, A.A., Saito, M., Makepeace, C., Permutt, M.A., Schlesinger, P., Mueckler, M., 2003. Wolframin expression induces novel ion channel activity in endoplasmic reticulum membranes and increases intracellular calcium. J. Biol. Chem. 278, 52755–52762.

Overstreet, D.H., Commissaris, R.C., De La Garza 2nd., R., File, S.E., Knapp, D.J., Seiden, L.S., 2003. Involvement of 5-HT1A receptors in animal tests of anxiety and depression: evidence from genetic models. Stress 6, 101–110.

Parra, A., Vinader-Caerols, C., Monleon, S., Simon, V.M., 1999. Learned immobility is also involved in the forced swimming test in mice. Psicothema 11, 239–246.

Philbrook, C., Fritz, E., Weiher, H., 2005. Expressional and functional studies of Wolframin, the gene function deficient in Wolfram syndrome, in mice and patient cells. Exp. Gerontol. 40, 671–678.

Riggs, A.C., Bernal-Mizrachi, E., Ohsugi, M., Wasson, J., Fatrai, S., Welling, C., Murray, J., Schmidt, R.E., Herrera, P.L., Permutt, M.A., 2005. Mice conditionally lacking the Wolfram gene in pancreatic islet beta cells exhibit diabetes as a result of enhanced endoplasmic reticulum stress and apoptosis. Diabetologia 48, 2313–2321.

Rotig, A., Cormier, V., Chatelain, P., Francois, R., Saudubray, J.M., Rustin, P., Munnich, A., 1993. Deletion of mitochondrial DNA in a case of early-onset diabetes mellitus, optic atrophy and deafness (DIDMOAD, Wolfram syndrome). J. Inherit. Metab. Dis. 16, 527–530.

Strom, T.M., Hortnagel, K., Hofmann, S., Gekeler, F., Scharfe, C., Rabl, W., Gerbitz, K.D., Meitinger, T., 1998. Diabetes insipidus, diabetes mellitus,

optic atrophy and deafness (DIDMOAD) caused by mutations in a novel gene (wolframin) coding for a predicted transmembrane protein. Hum. Mol. Genet. 7, 2021–2028.

Swift, M., Swift, R.G., 2000. Psychiatric disorders and mutations at the Wolfram syndrome locus. Biol. Psychiatry 47, 787–793.

Swift, R.G., Sadler, D.B., Swift, M., 1990. Psychiatric findings in Wolfram syndrome homozygotes. Lancet 336, 667–669.

Takeda, K., Inoue, H., Tanizawa, Y., Matsuzaki, Y., Oba, J., Watanabe, Y., Shinoda, K., Oka, Y., 2001. WFS1 (Wolfram syndrome 1) gene product: predominant subcellular localization to endoplasmic reticulum in cultured cells and neuronal expression in rat brain. Hum. Mol. Genet. 10, 477–484.

Takei, D., Ishihara, H., Yamaguchi, S., Yamada, T., Tamura, A., Katagiri, H., Maruyama, Y., Oka, Y., 2006. WFS1 protein modulates the free Ca(2+) concentration in the endoplasmic reticulum. FEBS Lett. 580, 5635–5640.

Threadgill, R., Bobb, K., Ghosh, A., 1997. Regulation of dendritic growth and remodeling by Rho, Rac, and Cdc42. Neuron 19, 625–634.

Torres, R., Leroy, E., Hu, X., Katrivanou, A., Gourzis, P., Papachatzopoulou, A., Athanassiadou, A., Beratis, S., Collier, D., Polymeropoulos, M.H., 2001. Mutation screening of the Wolfram syndrome gene in psychiatric patients. Mol. Psychiatry 6, 39–43.

Yamada, T., Ishihara, H., Tamura, A., Takahashi, R., Yamaguchi, S., Takei, D., Tokita, A., Satake, C., Tashiro, F., Katagiri, H., Aburatani, H., Miyazaki, J., Oka, Y., 2006. WFS1-deficiency increases endoplasmic reticulum stress, impairs cell cycle progression and triggers the apoptotic pathway specifically in pancreatic beta-cells. Hum. Mol. Genet. 15, 1600–1609.

Am J Physiol Endocrinol Metab 294: E668–E678, 2008.
First published January 29, 2008; doi:10.1152/ajpendo.00640.2007.

Ambient glucose levels qualify the potency of insulin myogenic actions by regulating SIRT1 and FoxO3a in C_2C_{12} myocytes

Taku Nedachi,[1] Akito Kadotani,[1,3] Miyako Ariga,[1,2] Hideki Katagiri,[2,3] and Makoto Kanzaki[1,4]

[1]*Division of Biomaterials, Tohoku University Biomedical Engineering Research Organization;* [2]*21st COE program "CRESCENDO", Graduate School of Pharmaceutical Sciences;* [3]*Division of Advanced Therapeutics for Metabolic Diseases, Center for Translational and Advanced Animal Research; and* [4]*Center for Research Strategy and Support, Tohoku University, Sendai, Japan*

Submitted 3 October 2007; accepted in final form 18 January 2008

Nedachi T, Kadotani A, Ariga M, Katagiri H, Kanzaki M. Ambient glucose levels qualify the potency of insulin myogenic actions by regulating SIRT1 and FoxO3a in C_2C_{12} myocytes. *Am J Physiol Endocrinol Metab* 294: E668–E678, 2008. First published January 29, 2008; doi:10.1152/ajpendo.00640.2007.—Nutrition availability is one of the major environmental signals influencing cell fate, such as proliferation, differentiation, and apoptosis, often functioning in concert with other humoral factors, including insulin. Herein, we show that low-serum-induced differentiation of C_2C_{12} myocytes is significantly hampered under low glucose (LG; 5 mM) compared with high glucose (HG; 22.5 mM) conditions, concurrently with nuclear accumulation of SIRT1, an NAD^+-dependent deacetylase, and FoxO3a, both of which are implicated in the negative regulation of myogenesis. Intriguingly, insulin appears to exert opposite actions, depending on glucose availability, with regard to the regulation of SIRT1 and FoxO3a abundance, which apparently contributes to modulating the potency of insulin's myogenic action. Namely, insulin exerts a potent myogenic effect in the presence of sufficient glucose, whereas insulin is unable to exert its myogenic action under LG conditions, since insulin evokes massive upregulation of both SIRT1 and FoxO3a in the absence of sufficient ambient glucose. In addition, the hampered differentiation state under LG is significantly restored by sirtinol, a SIRT1 inhibitor, whereas insulin abolished this sirtinol-dependent restoration, indicating that insulin can function as a negative as well as a positive myogenic factor depending on glucose availability. Taken together, our data reveal the importance of ambient glucose levels in the regulation of myogenesis and also in the determination of insulin's myogenic potency, which is achieved, at least in part, through regulation of the cellular contents and localization of SIRT1 and FoxO3a in differentiating C_2C_{12} myocytes.

forkhead box O; differentiation

SKELETAL MUSCLE CELLS have provided a useful model for exploring the molecular mechanisms involved in cellular differentiation (13), and insulin and insulin-like growth factors (IGFs) have been implicated in the process of myogenesis by activating the IRS-PI 3-kinase signaling pathway (7, 22, 25, 53) that also serves as a pivotal intracellular signal for exerting metabolic actions in mature skeletal muscle (9). However, despite our general understanding of the effects of ambient glucose levels on insulin responsiveness with regard to metabolic actions in skeletal muscle cells (37), the possible interrelationship between glucose and insulin acting on myogenesis remains to be clarified.

Skeletal muscle differentiation is a well-organized process governed by muscle-specific transcription factors belonging to the MyoD family, such as MyoD and myogenin (42), and the myocyte enhancer factor-2 (MEF2) family, such as MEF2A and MEF2C (35). In addition to these muscle-specific transcription factors, positively regulating myogenesis, the forkhead box O (FoxO) class of transcription factors, ubiquitously expressed in various cell types, has been shown to negatively regulate myogenesis (27). Insulin/IGF-induced repression of FoxO transcription factors, resulting from their nuclear exclusion in response to Akt-mediated phosphorylation, has been implicated in a key aspect of insulin/IGF actions not only for stimulating myogenesis but also for preventing muscle atrophy (21, 46).

Myogenesis is also directly influenced by the acetylation status of histones and nonhistone proteins including MyoD and MEF2, and class I and II histone deacetylases (HDACs) have been shown to regulate muscle gene expression by inhibiting MyoD and MEF2 factors (31, 33, 43). Recently, silent information regulator-2 (Sir2), a class III deacetylase originally characterized as controlling the life spans of animals in response to nutritional availability, was also identified to serve as a key regulator for myogenesis (14) via overexpression of SIRT1, the mammalian ortholog for Sir2, in C_2C_{12} myoblasts by strongly inhibiting differentiation into myotubes, whereas suppression of SIRT1 expression by RNA interference enhanced myogenesis (14).

Given the unique property of SIRT1 that the cofactor nicotinamide adenine dinucleotide (NAD^+) drives deacetylation activity, SIRT1 has been thought to serve as an energy and/or oxidation sensor, being directly involved in the nutritional regulation of gene transcription events in various tissues including skeletal muscle (38, 40, 45). Intriguingly, recent studies have also demonstrated that SIRT1 controls cellular functions by deacetylating FoxO transcription factors in response to various stimuli including nutritional availability (4, 36, 38). Thus, myogenesis is likely to be regulated cooperatively by SIRT1 serving as a sensor of the nutritional environment in concert with FoxOs serving as an insulin/IGF sensor in various situations in which glucose and insulin levels are fluctuating. However, no data are available on the potential interplay between ambient glucose levels and insulin in the regulations of SIRT1 and FoxOs, or on the regulation of myogenesis.

Address for reprint requests and other correspondence: M. Kanzaki, Center for Research Strategy and Support (CRESS), Tohoku University, 2-1 Seiryo-machi, Aoba-ku, Sendai 980-8575, Japan (e-mail: Kanzaki@tubero.tohoku.ac.jp).

The costs of publication of this article were defrayed in part by the payment of page charges. The article must therefore be hereby marked "*advertisement*" in accordance with 18 U.S.C. Section 1734 solely to indicate this fact.

To gain insight into these issues, we investigated the effects of ambient glucose levels on differentiation of C_2C_{12} myocytes and found the potency of insulin's myogenic action to be remarkably affected by extracellular glucose levels and that insulin exerts its maximum myogenic effect only in the presence of a relatively high level of glucose, whereas its potency is significantly compromised under low glucose (LG) conditions, a state in which massive upregulations of SIRT1 and FoxO3a are induced by insulin treatment. Thus, these findings reveal an important interplay between ambient glucose and insulin favoring alterations in the cellular contents of SIRT1 and FoxO3a, both of which are tightly coupled to the regulation of myogenesis.

MATERIALS AND METHODS

Materials. The Western blot detection kit (West super femto detection reagents) was obtained from Pierce Biotechnology (Rockford, IL). Dulbecco's modified Eagle's medium (DMEM), penicillin-streptomycin and trypsin-EDTA were purchased from Sigma Chemicals (St. Louis, MO). Cell culture equipment was from BD Biosciences (San Jose, CA). Calf serum (CS) and fetal bovine serum (FBS) were obtained from BioWest (Nuaille, France). Immobilon-P and anti-SIRT1 antibody were from Millipore (Bedford, MA). Anti-myosin heavy chain (MHC; MF20) and anti-myogenin (F5D) antibodies were obtained from Iowa Hybridoma Bank (University of Iowa, Iowa City, IA). Anti-phospho-S6 ($Ser^{235/236}$), anti-Akt, anti-phospho-Akt (Ser^{473}), and anti-phospho Akt (Thr^{308}) antibodies were purchased from Cell Signaling Technology (Danvers, MA). Anti-β-actin antibody was obtained from Sigma Chemicals. Unless otherwise noted, all chemicals were of the purest grade available from Sigma Chemicals.

Cell culture. Mouse skeletal muscle cell line C_2C_{12} myoblasts (54) were maintained in DMEM supplemented with 10% FBS, 30 μg/ml penicillin, and 100 μg/ml streptomycin (growth medium) at 37°C under a 5% CO_2 atmosphere. For biochemical study, the cells were grown on 4-well plates (Nalgen Nunc International, Rochester, NY) at a density of 1×10^5 cells/well in 5 ml of growth medium or on 6-well plates (BD Biosciences) at a density of 3×10^4 cells/well in 3 ml of growth medium. Three days after plating, cells had reached ~80–90% confluence (*day 0*). Differentiation was then induced by switching the growth medium to DMEM supplemented with 2% CS, 30 μg/ml penicillin, and 100 μg/ml streptomycin (differentiation medium). The differentiation medium was changed every 24 h. For the immunofluorescent staining study, cells were grown on 22-mm glass coverslips (C022221; Matsunami, Osaka, Japan) in 6-well plates.

Immunofluorescent studies. C_2C_{12} myoblasts were cultured on coverslips placed on 6-well plates. After differentiation, the cells were stimulated with 100 nM insulin for 60 min. Then, the cells were fixed with 2% paraformaldehyde in PBS (without Ca^{2+} and Mg^{2+}), followed by immunocytochemistry using anti-SIRT1 antibody (Millipore), and anti-mouse IgG antibody conjugated with Alexa 555 or Alexa 594 (Invitrogen, Carlsbad, CA). Images were monitored and analyzed using Olympus Fluoview FV1000 confocal microscopy and the associated application program, ASW v. 1.3 (Olympus, Tokyo, Japan).

Nuclear extract preparation. Nuclear extract preparation was performed as follows. Briefly, the cells were washed three times with PBS (-) and resuspended in *buffer A* (10 mM HEPES-OH, pH 7.9, 1.5 mM $MgCl_2$, 10 mM KCl). After a 20-min incubation on ice, the cells were destroyed with a vortex mixer (maximum speed), and the pellets were then collected. The pellets were resuspended in 50 μl of *buffer C* (HEPES-OH, pH 7.9, 420 mM NaCl, 1.5 mM $MgCl_2$, 0.2 mM EDTA, 25% glycerol) and then frozen (−80°C) and thawed twice. The supernatants were collected as nuclear extracts, and the protein concentration was measured and then stored at −80°C until Western blot analysis.

Immunoprecipitation. The cell lysates were prepared using Triton X-100-NP40 lysis buffer (50 mM Tris-Cl, 150 mM NaCl, 1 mM EDTA, 1% Triton X-100, 1% NP-40) and the protein concentrations of each sample were measured using a bicinchoninic acid assay (BCA) protein assay kit (Pierce). Five hundred micrograms of protein were mixed with 2 μg of anti-SIRT1 polyclonal antibody. The mixtures were incubated at 4°C for 3 h and continuously incubated in the presence of protein A-Sepharose. The immunoprecipitates were washed with Triton X-100-NP-40 lysis buffer three times. The adsorbed proteins were eluted with 1× Laemmli's buffer, boiled, and subjected to Western blot analysis.

Western blot analysis. The expression and phosphorylation of each protein were analyzed by Western blot analysis. In brief, the harvested cell lysates were subjected to 5% or 12% SDS-polyacrylamide gel electrophoresis (1:30 bis:acrylamide). Proteins were transferred to a PVDF membrane (Immobilon-P, Millipore), and the membranes were then blocked for 2 h at room temperature with 5% nonfat dry milk in Tris-buffered saline (TBS) containing 0.1% Tween-20. Immunostaining to detect each protein was achieved with a 1-h incubation with a 1:1,000 dilution of anti-SIRT1 antibody, anti-myosin heavy chain antibody, and anti-myogenin antibody. Specific totals or phosphoproteins were visualized after subsequent incubation with a 1:5,000 dilution of anti-mouse or rabbit IgG conjugated to horseradish peroxidase and a SuperSignal chemiluminescence detection procedure (Pierce Biotechnology). Protein concentrations were determined using a BCA assay. Three independent experiments were performed for each condition. Coomassie blue staining was also performed to assess the efficiency of protein transfer.

Real-time PCR. Fluorescence real-time PCR analysis was performed using a Light Cycler instrument and SYBR Green detection kit according to the manufacturer's instructions (Roche Diagnostics, Indianapolis, IN). PCR primers for measuring each of the secreted factors were as follows: for SIRT1, 5′-GAT CCT TCA GTG TCA TGG TT-3′ and 5′-GAA GAC AAT CTC TGG CTT CA-3′; for FoxO3a, 5′-TGC CTT GTC AAA TTC TGT C-3′ and 5′-TGC ACT AGC TGA ATA CAG TGA G-3′; for GAPDH, 5′-GGA GAA ACC TGC CAA GTA TGA-3′ and 5′-GCA TCG AAG GTG GAA GAG T-3′.

Glucose concentration assay. Glucose concentrations in the cultured media were measured using a determiner GLE kit (Kyowa Medex, Tokyo, Japan).

Statistical analysis. Statistical analysis was performed using one-way ANOVA followed by Tukey's multiple comparison test or Student's paired *t*-test for independent samples. Data are expressed as means ± SE unless otherwise specified.

RESULTS

Extracellular glucose influences low-serum-induced C_2C_{12} differentiation. To characterize the effects of extracellular glucose levels on myogenesis of C_2C_{12} cells, we first examined whether the glucose concentration in the low-serum differentiation medium (DMEM + 2% CS) affects C_2C_{12} differentiation. Under the LG (5 mM glucose) conditions, the process of myogenesis was obviously delayed and the number of well-developed myotubes was decreased compared with high glucose (22.5 mM glucose; HG) conditions on *day 4* of differentiation (Fig. 1*A*). We quantified differentiation status by counting the number of myotubes defined as multinuclear myotubes that contained more than 5 nuclei (Fig. 1*B*), as we previously reported (37). The effect of the extracellular glucose concentration on myogenesis was confirmed by Western blot analysis of differentiation marker proteins using anti-skeletal muscle type MHC and anti-myogenin antibodies, as not only were their expressions detected later, but their amounts were also